Endothelial cell-derived, secreted long non-coding RNAs *Gadlor1* and *Gadlor2* aggravate pathological cardiac remodeling via intercellular crosstalk

Merve Keles[1,2,3,#,*], Steve Grein[1,3*], Natali Froese[4], Dagmar Wirth[5], Felix A. Trogisch[1,2,3], Rhys Wardman[1,3], Shruthi Hemanna[1,3], Nina Weinzierl[1], Philipp-Sebastian Koch[6], Stefanie Uhlig[7], Santosh Lomada[3,8], Gesine M. Dittrich[1,3,†] , Malgorzata Szaroszyk[4], Ricarda Haustein[4], Jan Hegermann[9], Abel Martin-Garrido[1], Johann Bauersachs[4], Derk Frank[10, 11], Norbert Frey[3,12], Karen Bieback[7], Julio Cordero[13], Gergana Dobreva[3,13], Thomas Wieland[3,8] and Joerg Heineke[1,2,3]

[1]ECAS (European Center for Angioscience), Department of Cardiovascular Physiology, Medical Faculty Mannheim of Heidelberg University, Mannheim, Germany

[2]CFPM (Core Facility Platform Mannheim), Cardiac Imaging Center, Medical Faculty Mannheim of Heidelberg University, Mannheim, Germany

[3]DZHK (German Center for Cardiovascular Research), partner site Heidelberg/Mannheim, Germany

[4]Department of Cardiology and Angiology, Hannover Medical School, Hannover, Germany

[5]Helmholtz Center for Infection Research, Model Systems for Infection and Immunity, Braunschweig, Germany

[6]Department of Dermatology, Venereology and Allergology, University Medical Center and Medical Faculty Mannheim, Heidelberg University, Mannheim, Germany

[7]CFPM, FlowCore, Medical Faculty Mannheim of Heidelberg University, Mannheim, Germany

[8]ECAS, Department of Experimental Pharmacology, Medical Faculty Mannheim of Heidelberg University, Mannheim, Germany

[9]Institute of Functional and Applied Anatomy, Core Unit Electron Microscopy, Hannover Medical School, Hannover, Germany

[10]Department of Internal Medicine III, University Hospital Schleswig-Holstein, Kiel, Germany

[11]DZHK, partner site Hamburg/Kiel/Lübeck

[12]Department of Internal Medicine III, Medical Faculty Heidelberg, Heidelberg University, Heidelberg, Germany

[13]ECAS, Department of Cardiovascular Genomics and Epigenomics, Medical Faculty Mannheim of Heidelberg University, Mannheim, Germany

[#]Current Address: National Heart and Lung Institute, Faculty of Medicine, Imperial College London, London, United Kingdom

[†]Current Address: Department of Pharmacology and Toxicology, University Medical Center Göttingen, Göttingen, Germany

*These authors contributed equally.

Address for Correspondence:

Prof. Dr. Joerg Heineke

European Center for Angioscience (ECAS), Department of Cardiovascular Physiology,

Medical Faculty Mannheim, Heidelberg University

Ludolf-Krehl-Straße 7 – 11, 68167 Mannheim, Germany

Phone: +49 621 383 71850

Email: Joerg.Heineke@medma.uni-heidelberg.de

Short title: *Gadlor1* and *Gadlor2* lncRNAs in Cardiac Remodeling

Abstract

Pathological cardiac remodeling predisposes to heart failure. Here, we investigated two co-regulated long non-coding RNAs, termed *Gadlor1* and *Gadlor2*, which are upregulated in failing hearts of patients and mice. Cardiac overexpression of *Gadlor1* and *Gadlor2* aggravated myocardial dysfunction and enhanced hypertrophic and fibrotic remodeling in mice exposed to pressure overload. In turn, compound *Gadlor1/2* knock-out mice exerted markedly reduced myocardial hypertrophy, fibrosis and dysfunction, but more angiogenesis during short and long-standing pressure overload. Paradoxically, *Gadlor1/2* knock-out mice suffered from sudden death during prolonged overload, possibly due to cardiac arrhythmia. *Gadlor1* and *Gadlor2*, which are mainly expressed in endothelial cells (ECs) in the heart, where they induce pro-angiogenic gene-expression, are also secreted within extracellular vesicles (EVs). These EVs transfer *Gadlor* lncRNAs to cardiomyocytes, where they bind and activate calmodulin-dependent kinase II, and impact pro-hypertrophic gene-expression and calcium homeostasis. Therefore, we reveal a crucial EC-cardiomyocyte crosstalk as a potential future therapeutic target.

Key words: Extracellular vesicles; Hypertrophy; Heart failure; Calcium/calmodulin-dependent protein kinase type II; Cardiac angiogenesis

Introduction

Despite recent advances in therapeutic options, chronic heart failure is still one of the leading causes of global mortality, in part due to insufficient means to counteract maladaptive cardiac remodeling.[1-3] Cardiac remodeling comprises global changes in heart shape, reduced function and arrhythmia that are the consequence of cardiomyocyte hypertrophy, altered angiogenesis and myocardial fibrosis.[4, 5,6, 7] The majority of current therapeutic options target protein-coding genes; however, recent studies revealed the significance of non-coding transcripts in cardiovascular development and disease conditions.[5, 8, 9]

Long non-coding RNAs (lncRNAs) are a diverse group of non-coding transcripts that are longer than 200 nucleotides, and that in general do not encode for proteins.[10] Due to their complex structure, lncRNAs can act, for instance, as chromatin modifiers, affect protein functions, or alter mRNA stability or processing.[5] Thereby lncRNAs typically affect gene expression, alternative splicing or signaling pathways.[11, 12] Recent studies have identified several lncRNAs with crucial roles in cardiac remodeling and heart failure.[11, 13-16] Since non-coding transcripts are detectable in human body fluids such as in serum, circulating microRNAs (miRNAs) and lncRNAs are currently being investigated as clinical biomarkers, as well as for being paracrine mediators of cellular communication during stress conditions.[17-19] Intra-myocardial communication is a highly regulated process governing the complex physiology of the heart, whereby proper synchronization is required, for example, between endothelial cells (ECs) and cardiomyocytes, which rely on EC lined capillaries to provide nutrients and oxygen, but also paracrine factors regulating cardiomyocyte growth and function[20-22]. Cellular communication during pathological remodeling can be mediated by proteins, but also by the secretion and transfer of nanoscale extracellular vesicles (microvesicles and exosomes, termed small extracellular vesicles, EVs, in here) that carry non-coding RNAs and alter the behavior of recipient cells. [23-28,29,30] It is currently emerging that EVs transport lncRNAs between cells and thereby affect endothelial cell function, cardiac fibrosis and hypertrophy, but more work is needed.[26, 28, 31]

Here, we studied two related and secreted lncRNAs *Gadlor1* and *Gadlor2* (GATA-downregulated long non-coding RNA), which are jointly upregulated after endothelial deletion of GATA2.[32] We found that the expression of both *Gadlor* lncRNAs are significantly increased in hearts of mice after transverse aortic constriction (TAC), but also in the myocardium and serum of patients suffering from chronic heart failure. Moreover, our results revealed that *Gadlor1* and *Gadlor2* are secreted within EVs predominantly by cardiac ECs, from which they are mainly taken up by cardiomyocytes, although they also have autocrine/intracrine effects on ECs. In cardiomyocytes, *Gadlor1/2* impact calcium handling, hypertrophy and gene expression, while triggering anti-angiogenic effects in ECs. Our study reveals that secreted *Gadlor* lncRNAs aggravate cardiac remodeling but might protect from arrhythmias.

Results

Increased expression of *Gadlor* lncRNAs in cardiac pressure overload in mice and human failing hearts

Earlier observations by our group had identified two previously unknown lncRNAs *Gadlor1* and *Gadlor2*, which were markedly and jointly upregulated in cardiac ECs of endothelial-specific GATA2 knock-out mice.[32] *Gadlor1* (AK037972) and *Gadlor2* (AK038629) are located in close proximity to each other on mouse chromosome 16, and are embedded after exon1 of the *Lsamp* (limbic system-associated membrane protein) gene in its intronic region **(Fig. 1A)**. *Lsamp* is mainly expressed in the brain, and we did not detect significant *Lsamp* expression in the heart or cardiac ECs, and *Lsamp* expression patterns did not change in response to *Gadlor* knock-out in multiple organs **(Extended Data Fig. 1A-C)**. *Gadlor1* and *Gadlor2* are not matched with any known mouse peptides (BlastP, The National Center for Biotechnology Information (NCBI) database), and we verified that they are non-coding transcripts by using the CPAT algorithm to assess protein-coding probability **(Extended Data Fig. 1D)**. Cardiac *Gadlor1* and *2* expression is low in the direct postnatal period, but both transcripts become upregulated in parallel in the adult (2

months old) heart **(Fig. 1B)**. Cellular expression analysis among the main cell types in the heart revealed the highest *Gadlor1* and *Gadlor2* expression in ECs, followed by fibroblasts (FBs), while the lowest levels were detected in cardiomyocytes (CMs) **(Fig. 1C)**. In these analyses, *Gadlor 1* and *2* lncRNA levels were also significantly enriched in ECs compared to whole heart tissue.

Next, we assessed *Gadlor1/2* RNA levels in cardiac disease. Myocardial *Gadlor1* and *2* expression was markedly and jointly upregulated in the chronic phase (12 weeks) after TAC versus sham **(Fig. 1D)**. Predominant endothelial expression and the increased abundance during pressure overload were confirmed by fluorescent in situ hybridization **(Extended Data Fig. 1E-F)**.

The conservation of *Gadlor1/2* RNA between human, mouse and rat was analyzed with the EMBOSS-Water platform **(Extended Data Fig. 2)**, revealing high conservation between the three species. Importantly, *GADLOR1/2* expression was strongly induced in the myocardium of patients suffering from advanced heart failure **(Fig. 1E)**. We established an assay to specifically detect and quantify *GADLOR2* concentrations in human serum, which were significantly elevated in patients with heart failure due to aortic stenosis **(Fig. 1F)**. In this patient cohort, high *GADLOR2* serum concentrations were found mainly in patients with low left ventricular ejection fraction, and a negative correlation between these two parameters was identified **(Fig. 1G).** We were not able to establish a similar assay to quantify *GADLOR1* in human serum. Taken together, our results demonstrate *Gadlor1* and *Gadlor2* as lncRNAs that are co-upregulated in diseased mouse and human hearts.

***Gadlor* lncRNAs are enriched in EC-derived extracellular vesicles (EVs)**

Since *GADLOR2* was detectable in the serum of heart failure patients, and secreted EVs can contain lncRNAs,[26, 29] we hypothesized that *Gadlor*1/2 might be secreted within EVs. To test our hypothesis, the abundance of *Gadlor1/2* was analyzed in cultured primary mouse cardiac ECs and EVs collected and

purified from the supernatant of the ECs by ultracentrifugation **(Extended Data Fig. 3A)**. Initially, we characterized the isolated EVs with electron microscopy (EM), nanoparticle tracking analysis (NTA) and FACS. We found typical microvesicles and exosomes in EM, and the average size of the particles was slightly larger than 100 nm in diameter by NTA, which showed that they were in the range of microvesicles and exosomes (together called EVs in this study) **(Extended Data Fig. 3B-C)**. Flow cytometry assessment also confirmed the presence of CD63, CD9 and CD54 as common cell surface markers for EVs **(Extended Data Fig. 3D)**.

Interestingly, the absolute concentration of *Gadlor1/2* was markedly higher in cardiac EC-derived EVs compared to cardiac EC themselves **(Fig. 1H)**. EV *Gadlor1* and *2* RNA levels were not affected by proteinase K (PK), or by RNase A, which indicated *Gadlor1/2* were encapsulated within vesicles and protected from enzyme degradation **(Fig. 1I)**. Indeed, *Gadlor* lncRNAs were not protected upon direct incubation with PK and RNase A, or when EVs were dissolved by Triton-X, before RNase A was applied **(Fig. 1I)**. In addition to primary cardiac ECs, also C166 mouse ECs secreted *Gadlor* RNAs in EVs **(Extended Data Fig. 3E)**. Altogether, these results suggest that *Gadlor1* and *Gadlor2* are highly enriched and encapsulated in EC derived EVs.

Gadlor-KO mice are protected from cardiac hypertrophy and dysfunction during pressure-overload

To investigate the role of *Gadlor* lncRNAs, systemic *Gadlor* knock-out mice (*Gadlor*-KO) were generated by deletion of the respective region of mouse chromosome 16 (including *Gadlor* 1 and 2, since both were consistently jointly regulated in our analyses) by using a CRISPR-Cas9-based strategy **(Fig. 1A, Fig. 2A)**. Unchallenged *Gadlor*-KO mice were indistinguishable from their wild-type littermates (WT) based on appearance, body weight, heart weight, and baseline echocardiographic analysis **(Extended Data Fig. 4A-D)**. We detected, however, a mild increase in liver and decrease in brain weight in KO animals compared to WT littermates (**Extended Data Fig. 4E**).

The ablation of *Gadlor1/2* was confirmed in knock-out animals by qRT-PCR in different organs **(Fig. 2B).** We found *Gadlor1* and *Gadlor2* expression in heart, liver, brain, spleen and kidney, with the highest expression in the brain of WT mice **(Fig. 2B)**. To study the effect of *Gadlor1* and *Gadlor2* in cardiac remodeling during pressure-overload, WT and *Gadlor*-KO animals were subjected to TAC or sham surgery and subsequently monitored for 2 weeks **(Fig. 2C)**. The carotid flow was measured after 2 days of TAC in the right and left common carotid arteries (RCCA and LCCA, respectively) to evaluate the strength of the aortic constriction. The RCCA/LCCA flow ratio increased to a similar degree in both WT and *Gadlor*-KO animals, indicating comparable pressure overload **(Extended Data Fig. 4F-G).** We found a significant increase in heart weight to body weight (HW/BW) ratio after 2 weeks of TAC in both WT and *Gadlor*-KO compared to sham animals, however, less hypertrophy (i.e. a reduced HW/BW ratio) was observed in *Gadlor*-KO mice **(Fig. 2D)**. Additionally, heart-failure-induced pulmonary congestion was only observed in WT animals after TAC, whereas *Gadlor*-KO animals were protected **(Fig. 2E)**. In echocardiography, *Gadlor*-KO mice showed less cardiac systolic dysfunction, a markedly reduced left ventricle wall thickness (LVPW) and less chamber dilation (measured as left end-diastolic volume, LVEDV) compared to WT mice after TAC **(Fig. 2F-I)**.

Deletion of *Gadlor1* and *Gadlor2* alleviates cardiomyocyte hypertrophy and fibrosis *in vivo*

Sirius red staining revealed strongly diminished myocardial fibrosis in *Gadlor*-KO mice, which was supported by reduced cardiac *Col1a1* and *Col3a1* mRNA levels after TAC **(Fig. 2J-L).** A lower expression of *Nppa, Nppb*, a lower *Myh7/Myh6* RNA ratio, and a reduced cardiomyocyte cross-sectional confirmed blunted cardiac hypertrophy in *Gadlor*-KO animals compared to WT littermates after TAC **(Fig. 2M-O).** Additionally, Isolectin B4 (IB4) staining of capillaries revealed a substantial increase of capillary density in the myocardium of *Gadlor*-KO mice compared to WT animals after TAC **(Fig. 2N, P).** Together, our data

showed that deletion of *Gadlor*1/2 protected against cardiac hypertrophy, systolic dysfunction, capillary rarefaction and myocardial fibrosis during pressure overload.

Overexpression of *Gadlor1* and *Gadlor2* via EVs triggers cardiac dysfunction and fibrosis

To decipher the functional effect of increased *Gadlor1* and *Gadlor2* levels during pressure overload, we administered control EVs and *Gadlor*-enriched EVs to mouse hearts directly before TAC surgery by intra-ventricular injection (and concomitant cross-clamping of the aorta and pulmonary artery distal of the coronary vessels origin, to allow perfusion of the injected EVs through the coronaries). Control EVs were produced by purifying EC-derived EVs from the supernatant of control adenovirus (Ad.βgal) infected C166 mouse ECs, and *Gadlor1* and *Gadlor2* containing EVs were purified from the supernatant of Ad.*Gadlor1* and Ad.*Gadlor2* infected C166 ECs **(Fig. 3A)**. We detected significantly higher levels of myocardial *Gadlor1* and *Gadlor2* after 1 week of EV administration **(Fig. 3B)**. *Gadlor*-EV treated mice exerted a marked reduction of cardiac systolic function after 1-week and 2-weeks of TAC, as well as increased wall thickness compared to control EV treated animals (two cohorts were examined, cohort I and II, **Fig. 3A-E**). Histological analyses by Sirius red staining showed exaggerated myocardial fibrosis in *Gadlor*-EV treated mice, which was confirmed by qPCR of *Col1a1* and *Col3a1* mRNA expression in the myocardium **(Fig. 3F-G)**. Furthermore, increased expression of *Nppa* and *Nppb*, as well as a trend towards larger cardiomyocyte cross-sectional area verified increased hypertrophic remodeling in *Gadlor*-EV treated mice **(Fig. 3H-J)**. The myocardial capillary density was not changed between experimental groups **(Fig. 3K)**. We concluded that overexpression of *Gadlor1* and *Gadlor2* via administration of endothelial-derived EVs aggravated cardiac dysfunction and hypertrophy, and triggered fibrosis during pressure overload.

***Gadlor*-KO mice exert increased mortality during chronic pressure overload**

Next, we studied whether the protective effects of *Gadlor1/2* ablation were maintained during persisting long-term pressure overload **(Fig. 4A)**. Similar to our findings after 2 weeks of TAC, *Gadlor*-KO animals had a significantly reduced HW/BW ratio after 8-weeks of TAC compared to WT littermates, an improved systolic left ventricular function with reduced posterior wall thickness, an increased capillary density, diminished cardiomyocyte hypertrophy and markedly less fibrosis **(Fig. 4B-J)**. Despite retaining better systolic function and improved remodeling features, we observed a considerably higher mortality rate in *Gadlor*-KO mice starting between two and three weeks after TAC **(Fig. 4K)**. Interestingly, WT and KO animals were indistinguishable in terms of appearance, behavior and mobility after TAC operation, and death in *Gadlor*-KO mice was unexpected and sudden in nature, possibly due to cardiac arrhythmia.

***Gadlor1* and *Gadlor2* affect gene expression and angiogenic function in ECs**

Since ECs are the main cardiac cell-type expressing *Gadlor1/2*, and since we observed an increased capillary density in the myocardium of *Gadlor*-KO mice after two and 8 weeks of TAC (see above), we performed RNA sequencing from isolated WT and *Gadlor*-KO ECs after two weeks of TAC. The purity of ECs in our MACS-based isolation procedure is >90%.[33] The genome-wide transcriptome analysis via bulk RNAseq identified a total of 3355 differentially expressed (DE) genes between WT and *Gadlor*-KO, which are shown in the heatmap **(Fig. 5A)**. Gene ontology analysis from DE genes and RT-qPCR revealed and confirmed upregulation of angiogenesis, mitotic cell cycle and respiratory electron transport and downregulation of inflammatory response genes in *Gadlor*-KO EC after two weeks of TAC **(Fig. 5B-D)**. In addition, myocardial staining for Ki67 as a proliferation marker revealed more Ki67-positive EC in *Gadlor*-KO mice after TAC **(Fig. 5E-F)**. In turn, overexpression of *Gadlor1* and *Gadlor2* by adenovirus in C166 mouse ECs blunted the increase in EC sprouting activity during FGF2 stimulation and reduced sprouting further in the presence of TGFβ in comparison to Ad.β*gal* (control) infected cells **(Fig. 5G-H)**. In summary, *Gadlor* lncRNAs exert anti-angiogenic properties in ECs.

1

2 **Cardiac FB of *Gadlor*-KO mice induce less fibrosis-associated genes after TAC**

3 Based on our findings, cardiac fibroblasts (FBs) exerted the second highest *Gadlor* lncRNAs expression after
4 ECs in the myocardium **(Fig. 1C).** To study the reason for decreased fibrosis in hearts
5 upon *Gadlor* knock-out after TAC, we performed bulk RNAseq from isolated cardiac FBs after two weeks
6 of TAC. The purity of cardiac FBs in our MACS-based isolation procedure is >90%.[33] Genome-wide analysis
7 revealed a total of 915 downregulated and 998 upregulated genes in *Gadlor*-KO FBs compared to WT mice
8 after TAC, which are shown in a heatmap in **Extended Data Fig. 5A**. Amongst these, we detected a strong
9 downregulation of mainly ECM organization and growth factor associated genes (confirmed by RT-qPCR:
10 *Fgfr1, Igf1, Col1a1, Col3a1, Col6a1*) **(Extended Data Fig. 5B-D)**. Additionally, genes related to the
11 regulation of angiogenesis, blood vessel and endothelium development were upregulated in *Gadlor*-KO
12 FBs, which suggested a contribution of FBs to the enhanced angiogenesis observed in *Gadlor*-KO mice
13 upon overload. The increased expression of *Angpt2, Efna1, Aurkb, Dll1* in cardiac FBs from *Gadlor KO* mice
14 was confirmed by RT-qPCR **(Extended data Fig. 5C)**. Upon adenoviral overexpression of *Gadlor1* and
15 *Gadlor2* followed with phenylephrine (PE) stimulation, neonatal rat cardiac fibroblasts (NRFB), in turn,
16 exerted a decreased expression of *Angpt2*, and an increased expression of *Col1a1* and *Col3a1*, but no
17 differential expression was observed for *Col4a1* or *Col6a1* **(Extended Data Fig. 5E)**. We concluded that
18 *Gadlor* lncRNAs trigger pro-fibrotic gene expression in cardiac FBs.

19

20 ***Gadlor* lncRNAs are transferred to cardiomyocytes via EC-derived EVs**

21 Since *Gadlor1* and *Gadlor2* were mainly secreted by ECs, we reasoned that these lncRNAs might exert
22 paracrine effects due to EV-mediated transfer into cardiomyocytes, where they could affect contraction,
23 arrhythmia, or hypertrophy. To analyze whether *Gadlor*1/2 are transferred from ECs to cardiomyocytes,

we initially overexpressed *Gadlor1/2* by adenovirus in C166 mouse ECs, and purified EVs from the supernatant of these cells **(Fig. 6A)**. We confirmed the enhancement of *Gadlor1/2* expression in EVs upon *Gadlor1/2* overexpression versus control EVs **(Fig. 6B)**. The collected EVs were transferred either to neonatal rat cardiomyocytes (NRCMs) or fibroblasts (NRFBs). RT-qPCR analysis showed a significantly higher abundance of *Gadlor1/2* in NRCMs incubated with *Gadlor*-EVs compared to samples incubated with control-EVs or cardiomyocytes without any EV treatment, which indicated that EVs were taken up by cardiomyocytes **(Fig. 6C)**. *Gadlor* lncRNAs were also transferred from EC to cardiomyocytes by control EVs, since higher cardiomyocyte *Gadlor1/2* levels were observed after control EV compared to non-EV treatment. Additionally, a mild increase in both *Gadlor1* and *Gadlor2* abundance was also observed in NRFBs after incubation with *Gadlor* EVs, however, at a much lower degree compared to NRCMs **(Fig. 6C)**. We visualized the uptake of the fluorescently labelled (PKH67) EVs into recipient cardiomyocytes, which was analyzed with confocal microscopy after 6 hours and 24 hours **(Fig. 6D)**. 3D imaging by confocal Z-stacks confirmed that EVs were internalized into the recipient cardiomyocytes rather than being attached to the surface **(Extended Data Video 1)**.

Furthermore, we performed co-culture experiments with isolated *Gadlor*-KO cardiomyocytes (lacking endogenous *Gadlor1/2* expression) and WT mouse cardiac endothelial cells (MCEC, on cell culture inserts, which allow the transfer of EVs, due to a pore size of 1 μm) for 48 hours **(Fig. 6E)**. *Gadlor*-KO cardiomyocytes were used to exclude confounding effects of endogenous *Gadlor1/2* expression with exogenous *Gadlor1/2* uptake from EC-derived EVs. As expected, we did not find any *Gadlor1/2* expression in isolated *Gadlor*-KO cardiomyocytes when they were kept in monoculture, whereas we detected *Gadlor1* and *Gadlor2* after co-culture with WT MCECs **(Fig. 6F)**. This suggested that *Gadlor1/2* were transferred into *Gadlor*-KO cardiomyocytes from WT MCECs, possibly via EV-mediated cell-to-cell transfer. MCECs that were co-cultured with *Gadlor*-KO cardiomyocytes also exerted an increase of *Gadlor1/2* expression **(Fig. 6F)**, which might suggest a possible feedback mechanism between cardiomyocytes and ECs. The addition

of GW4869 as inhibitor of exosome (i.e. small EV) generation into the co-culture system ablated the transfer of EC derived *Gadlor1/2* to KO cardiomyocytes as well as the putative feedback mechanisms, suggesting that both might depend on small EVs **(Fig. 6G)**. Next, we wanted to assess whether WT cardiomyocyte depend on ECs for *Gadlor1/2* expression. Indeed, inclusion of GW4869 into co-culture of WT cardiomyocytes with WT MCECs, markedly reduced *Gadlor1/2* levels in the cardiomyocytes. This indicated that ECs provide *Gadlor1/2* to cardiomyocytes and might thereby relay paracrine signals to these cells **(Fig. 6H)**.

Sub-cellular fractionation studies to localize *Gadlor* lncRNAs following EV-mediated transfer showed that *Gadlor1* and *Gadlor2* were detected in the cytosol and in a bit higher level in the nucleus of recipient cardiomyocytes **(Fig. 6I)**. Overall, endothelial-derived *Gadlor1/2* containing EVs are mainly taken up by cardiomyocytes, where they might act in the cytosol as well as in the nucleus. Cardiac FBs may mainly rely on their own cellular *Gadlor1/2* expression.

***Gadlor* lncRNAs bind to calcium/calmodulin-dependent protein kinase type II in cardiomyocytes**

LncRNAs can interact with proteins to affect their regulatory functions.[34] Even though cardiomyocytes showed the least endogenous levels of *Gadlor* lncRNAs, we still observed strong effects in cardiomyocytes (e.g. reduced hypertrophy and potentially arrhythmia) after *Gadlor1/2* deletion upon pressure overload. To decipher this further, we aimed at identifying the binding partners of *Gadlor1/2* in cardiomyocytes by performing RNA antisense purification coupled with mass-spectrometry (RAP-MS) in HL1 cardiac muscle cells after overexpression of *Gadlor1/2* **(Fig. 7A)**. Interestingly, we found calcium/calmodulin-dependent protein kinase type II, delta (CaMKIIδ) as the most significant binding partner of *Gadlor1/2* **(Fig. 7B)**. Next, we confirmed the interaction between CaMKII and *Gadlor1/2* with native RNA immunoprecipitation (RIP), i.e. immunoprecipitation of CaMKII, followed by qRT-PCR to detect *Gadlor1* and *Gadlor2* **(Fig. 7C)**. We then

investigated whether *Gadlor1/2* modulates CaMKII function by assessing phospholamban Threonine-17 (Thr17) phosphorylation, which is mediated directly by CaMKII. Indeed, we found reduced and increased Thr17 phospholamban phosphorylation in *Gadlor*-KO mice or *Gadlor*-EV treated mice after TAC, respectively **(Fig. 7D-G)**. This indicated that *Gadlor1/2* might promote CaMKII activation in cardiomyocytes.

Since *Gadlor* lncRNAs had influenced cardiac function, and CaMKII was identified as binding partner, which has a known role in cardiomyocyte excitation-contraction coupling, we investigated cardiomyocyte contractility and calcium dynamics with the CytoCypher High-Throughput (HT) system (Ionoptix) in isolated adult cardiomyocytes after one week of TAC. Interestingly, during measurements, a considerably higher number of *Gadlor*-KO cardiomyocytes with arrhythmic behavior was detected compared to WT cardiomyocytes **(Fig. 7H)**. Sarcomeric length traces **(Fig. 7I)** indicated that *Gadlor*-KO cardiomyocytes exhibited double contractions even though they were paced with electrical field stimulation, in which each stimulation usually results in a single contraction.

Interestingly, *Gadlor*-KO cardiomyocytes displayed a much slower re-uptake of calcium into the sarcoplasmic reticulum (SR), which led to prolonged calcium transients. We also observed an increased calcium peak height in *Gadlor*-KO cardiomyocytes **(Fig. 7J-K).** Additionally, while sarcomere shortening and its timing were not significantly affected, cardiomyocyte relaxation was delayed **(Fig. 7L)**. Treatment of adult mouse cardiomyocytes with *Gadlor1/2* enriched versus control EC-derived EVs, in turn, led to augmented sarcomere shortening and especially faster cardiomyocyte relaxation **(Fig. 7M)**. While calcium peak height was not changed, a faster diastolic calcium re-uptake was detected by a decreased tau value **(Fig. 7N)**. Collectively, *Gadlor*-KO myocytes displayed an enhanced propensity to arrhythmic beating, slower diastolic relaxation and slower calcium re-uptake into SR, which entailed increased intracellular calcium levels. Overexpression of *Gadlors1/2,* in turn, led to increased sarcomere shortening, faster cardiomyocyte relaxation and faster re-uptake of calcium into the SR. These effects were partially rescued

upon KN93 (CaMKII inhibitor) treatment **(Fig. 7O)**, which decreased the sarcomere shortening and increased the time needed for re-uptake of calcium into the SR (tau) in *Gadlor*-EV treated cardiomyocytes, indicating that *Gadlor1/2* exert their effects on excitation-contraction coupling at least in part through CaMKII activation.

Gadlor1 and _Gadlor2_ promote pro-hypertrophic and mitochondrial gene-expression in cardiomyocytes

Since *Gadlor1/2* were in part localized in cardiomyocyte nuclei after their transfer **(Fig. 6I)**, we hypothesized that they might also affect gene expression in these cells. Comprehensive transcriptome analysis after two weeks of TAC between isolated WT and *Gadlor*-KO cardiomyocytes revealed that 2492 genes were up-, while 2956 were downregulated after ablation of *Gadlor1/2* as shown in the heatmap in **Fig. 8A**. Functional annotation of DE genes showed that genes related to vasculature development, ECM organization and regulation of cytokine production were upregulated **(Fig. 8B)**, while mitochondrial organization, TCA cycle and cardiac muscle contraction/hypertrophy related genes were downregulated in *Gadlor*-KO cardiomyocytes **(Fig. 8B)**. We confirmed the upregulation of *Il6, Tlr9, Col15a1, Col14a1, Adam8* mRNAs, and the downregulation of *Camk2d, Gata4, Actn2, Mfn2* mRNAs in Gadlor-KO cardiomyocytes after TAC by RT-qPCR **(Fig. 8C-D)**. To rule out a reduced number of mitochondria as a reason for the downregulation of mitochondrial genes, we assessed the mitochondrial-to-nuclear DNA ratio, but detected no changes in *Gadlor*-KO versus WT mice, indicating a similar number of mitochondria under both conditions **(Fig. 8E)**. We next assessed the effects of *Gadlor1/2* overexpression on cardiomyocyte gene-expression after PE stimulation **(Fig. 8F)**. *Gadlor1/2* overexpres sion in large parts revealed opposite effects of what was found in *Gadlor*-KO cardiomyocytes, for example it promoted the expression of genes assigned to the GO-class “cardiac muscle contraction” (*Gata4*, *Camk2d*, *Rcan1.4*), which mainly exert pro-hypertrophic function in cardiomyocytes. These effects were partially reversed

upon treatment with KN93, indicating CaMKII-dependent effects of *Gadlor1/2* on pro-hypertrophic (and other) gene expression.

Comparing the effects of *Gadlor* knock-out in the different cardiac cell types after TAC revealed a strong overlap among upregulated and downregulated genes in FBs, ECs and cardiomyocytes **(Extended Data Fig. 6)**. For example, *Gadlor* knock-out led to the upregulation of energy-coupled proton transport mitochondrial genes, actin filament associated genes, and mitotic cell cycle related genes in all three cell types, in addition to the upregulation of cardiac muscle contraction and blood vessel morphogenesis genes in two cell types. On the other hand, genes related to the negative regulation of cell differentiation, cartilage development and the regulation of membrane potential were downregulated in all three cell types, while genes related to cell migration, inflammation, extracellular matrix organization, heart contraction, calcineurin/NFAT signaling and mitochondrial organization were downregulated in at least two of the cell types **(Extended Data Fig. 6)**. Therefore, *Gadlor1/2* effects on gene expression contain common, but also unique targets in different cardiac cell types. The findings of this study are graphically summarized in **Extended Data Fig. 7**.

Discussion

Here, we describe two lncRNAs (termed *Gadlor1* and *Gadlor2*) as central regulators of cardiac failure during pressure overload. *Gadlor1* and *Gadlor2* were jointly upregulated in mouse and human failing hearts. In the serum of patients with aortic stenosis, high *GADLOR2* levels were associated with a low ejection fraction. Accordingly, enhanced experimental *Gadlor1/2* expression in mouse hearts triggered aggravated heart failure, myocardial hypertrophy and fibrosis, while combined *Gadlor*-KO mice were protected from cardiac dysfunction, fibrosis and vascular rarefaction during short and persisting pressure overload. Paradoxically, despite retaining better heart function and remodeling features, the complete

lack of *Gadlor* lncRNAs during chronic, persisting pressure overload entailed sudden death, most likely due to arrhythmia.

Among the different cell types in the myocardium, we found the highest *Gadlor1/2* expression in ECs, where reduced *Gadlor1/2* levels entailed an increased capillary density and cell proliferation after TAC. Importantly, enhanced myocardial angiogenesis was reported to promote cardiac function during pressure overload.[20, 22] *Gadlor1/2* overexpression in isolated ECs reduced angiogenic activity, indicating that *Gadlor* lncRNAs inhibit angiogenesis in ECs in a cell autonomous manner. Because lncRNAs often exert their effects by modifying gene expression, we performed transcriptome profiling by RNA sequencing in cardiac ECs after TAC. Indeed, we found that upon *Gadlor1/2* deletion, EC upregulate genes related to angiogenesis, cell cycle and mitosis. Besides this cell-autonomous role, *Gadlor*-KO mice also exerted an increased expression of proangiogenic genes in cardiomyocytes and FBs during TAC, which are both known to affect angiogenesis in a paracrine manner.[20, 21, 35, 36]

In addition to ECs, cardiac FBs exhibited high levels of *Gadlor1/2* expression in the heart. Transcriptomic profiling in cardiac FBs revealed the downregulation of many extracellular matrix-organizing genes, including pro-fibrotic growth factors, their receptors as well as matrix proteins themselves in *Gadlor*-KO mice. Our data imply that the pro-fibrotic role of *Gadlor1* and *Gadlor2* are mediated by their direct effect on gene expression in cardiac FBs. Increased and decreased fibrosis will likely play a major role in reduced and improved heart function during TAC in mice with enhanced or ablated *Gadlor* expression, respectively.

Remarkably, *Gadlor1/2* are mainly secreted within EVs from ECs. This finding indicated a potential paracrine role of *Gadlor* lncRNAs in the heart. Indeed, EVs were reported to contain mainly miRNAs, but also lncRNAs and mRNAs, and to protect these RNA species from degradation by extracellular RNases.[37] EVs might thereby play a role in intercellular communication, especially during stress stimulation or disease, when their production is typically upregulated.[38] In cell culture experiments, we found an effective uptake of *Gadlor1/2* from endothelial-derived EVs in neonatal and adult cardiomyocytes. When adult

cardiomyocytes from *Gadlor*-KO mice that naturally could not upregulate intrinsic *Gadlor1/2* lncRNA expression were co-cultured in a two-chamber system (allowing the transfer of EVs, but not cells between the compartments) with wild-type ECs, these ECs in the upper well increased *Gadlor1/2* levels in the knock-out cardiomyocytes at the bottom well, an effect that was blunted by inhibition of small EV generation. In addition, the co-cultured WT ECs markedly upregulated their *Gadlor1/2* expression compared to when they were cultured alone, which was also blunted by EV inhibition. Perhaps even more importantly, when WT ECs and WT cardiomyocytes were co-cultured, EV-inhibition strongly reduced *Gadlor1/2* levels in the WT cardiomyocytes. This demonstrated that EC-derived EVs are crucial to provide *Gadlor1/2* to cardiomyocytes, in which they regulate calcium cycling as well as gene-expression. Our results therefore indicated a reciprocal intercellular signaling circuit between ECs and cardiomyocytes, whereby ECs provide *Gadlor* lncRNAs within EVs to cardiomyocytes, which signal back to ECs by currently unknown (perhaps EV based) mechanisms to indicate insufficient *Gadlor1/2* levels, when necessary. Indeed, signal responsive EV release had been previously described.[38] In conclusion, *Gadlor1/2* exert a strong effect in intercellular communication in the heart during pathological overload, on one hand by directly serving as intercellular messenger between ECs and cardiomyocytes, and on the other hand by regulating the gene-expression of secreted growth factors in cardiomyocytes, ECs and FBs, thereby affecting, for instance, angiogenesis and fibrosis.

In cardiomyocytes, *Gadlor1/2* lncRNAs are taken up from ECs and localize to the cytosolic as well as to the nuclear compartment. Accordingly, we identified CaMKII as one of the binding partners of *Gadlor1/2* in cardiomyocytes, which localizes to both compartments and is activated mainly by calcium/calmodulin, autophosphorylation and oxidation or S-nitrosylation.[39] Its activity is known to be about 3-fold upregulated in failing human hearts.[40] In cardiomyocytes, CaMKII promotes on one hand maladaptive features such as hypertrophy and fibrosis by phosphorylating HDAC4, leading to de-repression of MEF2-dependent, pro-hypertrophic gene expression.[41, 42] On the other hand, it has adaptive functions, for example, it promotes

calcium re-uptake into the SR by phosphorylating phospholamban at Thr17.[43-45] Because *Gadlor1/2* bind CaMKII and *Gadlor*-KO mice exerted reduced, while *Gadlor*1/2 overexpression led to enhanced Thr17 phosphorylation, we concluded that the *Gadlor* lncRNAs might promote CaMKII activation in a feed-forward loop in cardiomyocytes during pathological overload. Decreased CaMKII activity could account for the improved cardiac remodeling features (i.e. reduced hypertrophy and improved systolic heart function) in *Gadlor*-KO mice, and at the same time slow down calcium re-uptake into the SR, leading to increased cytosolic calcium levels with pro-arrhythmic activity. Indeed, upon *Gadlor1/2* overexpression, pharmacological CaMKII inhibition partially reversed pro-hypertrophic gene expression and reversed increased calcium cycling in isolated cardiomyocytes. Besides facilitating CaMKII activity by direct protein binding, *Gadlor1/2* also appear to promote *Camk2d* expression at the mRNA level. As another pro-hypertrophic gene, *Gata4* is also positively regulated by *Gadlor1/2* in cardiomyocytes. Although details how *Gadlor1/2* directly regulate gene-expression in the cardiomyocyte nucleus will have to be addressed in future studies, this could work through binding to the chromatin reader protein GLYR1 (also known as NDF, NPAC or NP60), which we also found as direct binding partner of *Gadlor1/2* and that is strongly involved in the regulation of cardiomyocyte gene-expression during differentiation by binding to the gene body of actively transcribed genes, often together with GATA4.[46]

Considering their dichotomous role, *Gadlor1/2* inhibition in cardiomyocytes might not be a suitable therapeutic strategy during persisting cardiac overload. Even though this would lead to inhibition of hypertrophy, there might be the danger of arrhythmia. On the contrary, targeted inhibition of *Gadlor1/2* effects in ECs and FBs could be beneficial, as it would entail increased angiogenesis and reduced FB-mediated fibrosis, which according to our data are likely the main underlying reasons for improved heart function in *Gadlor*-KO mice. Although more work is needed, we suggest that the inhibition of *Gadlor* effects in cardiac non-myocytes might be a promising strategy to treat heart failure in the future.

Limitations

Although we identified CaMKII as direct target of *Gadlor1* and *2* in cardiomyocytes that crucially affect calcium cycling and hypertrophy, we did so far not identify the direct targets of *Gadlor* lncRNA in ECs or FBs, which will be our aim in future studies. Furthermore, we cannot prove the intercellular transport of *Gadlor1/2* in the heart *in vivo* at this point, as the detection of EV transfer of specific content between cells in the whole organ is methodologically impossible. While we have identified a crucial role of *Gadlor1/2* under pathological conditions, their role in normal physiology remains unclear. We envision *Gadlor1/2* might serve to fine-tune the link between capillary and cardiomyocyte growth and function also in the absence of pathology in the adult heart, but this needs experimental validation in the future.

Methods

Human Samples

Studies on human heart tissue samples were approved by the Institutional Ethical Board of Massachusetts General Hospital (US), where samples were collected from patients with end-stage heart failure undergoing cardiac transplantation.[47] Control heart tissue samples were obtained from healthy organ volunteers when the organ was not eligible for transplantation, or from the victims of traffic accidents. Human serum samples were obtained from healthy blood donors, or from aortic stenosis patients before replacement of the aortic valve (clinical data are available in **Supplementary Table 1**), where all donors were provided a written informed consent for the collection and use of samples, that had received approval from the Institutional Review Board of Christian-Albrechts-Universität Kiel (File number: A174/09).

Measurement of GADLORs in Human Serum Samples

Human serum samples were collected on the day before Transcatheter Aortic Valve Implantation (TAVI). Serum-RNA was extracted using miRNeasy serum/plasma kit (#217184; Qiagen) based on the manufacturer's instructions. LncRNA levels were normalized by the addition of 2 µl of TATAA universal RNA Spike (#RS10SII; Tataa Biocenter) prior to RNA isolation. RNA was transcribed to cDNA (#K1652; Maxima H Minus First Strand cDNA Synthesis Kit; Thermo Fisher) and analyzed with TaqMan Non-coding RNA Technology (#4369016) using custom-specific TaqMan Gene Expression Assay (#43331348, ID: APPRKET und APRWEYP; Thermo Fisher). For quantitative RT-PCR, Stratagene's MX4000 multiplex qPCR system was used.

Animal Models and Studies

All studies including the use and care of animals were performed with the permission of the Regional Council Karlsruhe and the Lower Saxony State Office for Consumer Protection and Food Safety, Germany, with approved protocols 35-9185.81/G-144/18, I-22/03, 33.9-42502-12-10/0016, 33.19-42502-04-14/1403 and 33.8-42502-04-16/2356. Female and male animals were used in similar proportions throughout the study, except for the experiments in Figure 3, where only male mice were used.

Wildtype ICR/CD1 mice were in-bred in-house and C57BL/6N mice were obtained from Janvier Labs (Le Genest-Saint-Isle, France). Animals were maintained in a temperature-humidity controlled (22± 2°C and 35-60% humidity), 12-h dark-light cycled room with unlimited access to water and standard food.

Systemic *Gadlor* knock-out mice (*Gadlor*-KO) were generated by deletion of the respective region of mouse chromosome 16 using a CRISPR-Cas9-based strategy to achieve homozygous deletion. Briefly, embryonic stem cells (G4 line)[48] were transfected with gRNAs LNC1-01 (target sequence: 5'-TTGTACATGAGCGGTTGTAG) and LNC2-01 (target sequence 5'-AGTATACAGGGGGTTACCAT) as well as in

vitro transcribed CAS9-GFP mRNA. GFP-expressing cells were sorted and single-cell derived clones were established. 5 out of 72 analyzed clones showed extensive deletions between the gRNA target sites. Clones 1-37 comprised a deletion between 39,995,533 – 40,004,426 on one chromosome 16 allele. This clone was injected into C57BL/6 blastocysts to generate a transgenic mouse line which was then further crossed to achieve a homozygous deletion.

Pressure overload was induced in 8-10 weeks old mice by transverse aortic constriction (TAC) and maintained for 2 weeks for short-term and 8-12 weeks for long-term studies. Analgesia (0.1 mg/kg buprenorphine) was provided by subcutaneous injection. Tracheal intubation was followed by upper thoracotomy to visualize the aortic arch, which was tied with a 7-0 silk ligature around a 26-gauge needle that was removed immediately after secured constriction. Mice were injected with 0.1 mg/kg atropine, and the chest wall was closed with suture then followed by closure of the skin with surgical glue. The mice were ventilated with 2% isoflurane throughout the procedure. For postoperative care, additional analgesia was provided in drinking water for the following 5 days. To assess the mortality rate, mice were followed and inspected daily after TAC. Sham-operated animals were treated with the same procedure and medications, but no constriction was applied to the aortic arch. Mice were monitored with echocardiography before, and during pressure overload studies for assessment of cardiac function.

Transthoracic Echocardiography

Echocardiography was performed with 1% isoflurane anesthesia. Mice were dorsally placed on a heated table to maintain the body temperature during the procedure while the ECG and the respiration rate were recorded continuously. Echocardiography was recorded with a linear 30-40 MHz transducer (MX-550D) and the Vevo 3100 system (VisualSonics, Toronto, Canada). Data were analyzed with the Vevo Lab 5.5.0 software.

Left Ventricle and Apical four Chamber View. Parameters were recorded in B-mode and M-mode in both parasternal long-axis (PSLAX) and short-axis (SAX) view at the papillary muscle level. Left-ventricular posterior wall thickness and left-ventricular end-diastolic volume were used to characterize LV microanatomy (LVPW and LVEDV) and the change of LV diameter length from end-diastole (LVID) to end-systole was used to assess contractility and to calculate LV ejection fraction and fractional shortening (LV-EF and LV-FS), which were measured with the PSLAX mode in the analysis. B-mode tracing in the apical four-chamber view was recorded at the atrioventricular valve level with pulse wave-Doppler (PW-Doppler) and tissue-Doppler measurements.

Carotid flow measurement. To evaluate the degree of aortic constriction during TAC surgery, the peak velocity of flow in the right and left common carotid arteries (RCCA and LCCA) were measured 2 days after surgery with PW-Doppler at the level of carotid bifurcation to calculate the ratio of RCCA/LCCA flow.

Organ Harvest

At the end of the experiment, mice were weighed and euthanized to collect the heart, lungs and liver. Organs were washed in cold PBS to remove the blood, and additionally, the heart was washed in 0.5% (w/v) KCl in PBS. The heart was transversely cut into half, and the upper layer was immediately embedded into OCT for histological analysis while the other half was snap frozen.

Histology

OCT-embedded organs were sectioned into slices of 7 µm and 12 µm for immunofluorescence and Picro-Sirius red staining, respectively. Briefly, for immunofluorescence tissue sections were fixed with 4% PFA followed by permeabilization with 0.3% Triton-X in PBS and blocking with 3% BSA. Primary and secondary

antibodies that were used are listed in **Supplementary Table 3**. Samples were visualized with Leica DMi8 Fluorescence microscope. Images were analyzed with Leica Application Suite X (LAS X) 3.7.

Sirius red staining was performed by fixing the tissue samples with 100% ice-cold acetone, and by following the standard protocol. Tissue sections were scanned with Zeiss Axio Scan.Z1. Images were analyzed with ZEN 2.6 Blue Edition, Carl Zeiss.

Isolation and Culture of Juvenile Mouse Endothelial Cells (mECs)

Hearts from 7-12 days old mice were collected and washed in ice-cold DMEM high-glucose to clean and remove the atria. The minced tissue was transferred into 5 ml of enzyme solution (for 3-4 hearts) and incubated with collagenase I (500 U/ml, Worthington - LS004176) and DNase I (150 U/ml, Worthington - LS002139) in HBSS (without Ca and Mg). After digestion, the lysate was washed with FCS and passed through a 70 µm cell strainer. The washed lysate was incubated with CD31 antibody (BD, 553370) coupled to Dynabeads (Invitrogen, 11035) for the first step of isolation, before the cells were plated on 0.5% gelatinized plates. For culturing, cells were maintained for 3-4 days until they reached 80-90% confluency. During the first passage, further purification of cells was achieved by incubation with CD102 antibody (BD, 553370) coupled Dynabeads. Primary endothelial cells were maintained in DMEM with 20% FCS supplemented with non-essential amino acids and sodium pyruvate and passaged up to P3 for experiments.

Isolation of Adult Mouse Endothelial Cells, Fibroblasts and Cardiomyocytes

Isolation of endothelial cells and fibroblasts from adult mouse hearts was performed with MACS-magnetic beads from Miltenyi Biotec. Briefly, heart tissue was washed in ice-cold PBS and minced into small pieces before incubating in enzyme solution (collagenase I (500 U/ml, Worthington - LS004176) and DNase I (150

U/ml, Worthington - LS002139) in RPMI 1640 (Thermo Fischer Scientific: 31870025)). Digested tissue samples were passed through a 70 µm cell strainer and washed with FCS, and MACS buffer with BSA (Miltenyi Biotec, 130-091-222). After multiple washing steps, the tissue lysate was incubated with CD146 microbeads (Miltenyi Biotec, 130-092-007) before being passed through magnetic columns (Miltenyi Biotec, MS columns 130-042-201) for positive selection of endothelial cells (EC). The flow-through was incubated with feeder removal microbeads (Miltenyi Biotech, 130-095-531) and eluted after multiple washing steps to collect fibroblasts (FB). Isolated cells were stored as frozen cell pellet for later RNA or protein isolation for corresponding experiments.

Isolation of adult cardiac myocytes was achieved by using a Langendorff perfusion system.[49] Briefly, immediately after excision, the heart was placed into ice-cold 1x perfusion buffer (10x stock: 1130 mM NaCl ,47 mM KCl, 6mM KH_2PO_4, 6 mM Na_2HPO_4, 12 mM $MgSO_4.7H_2O$, 120 mM $NaHCO_3$, 100 mM $KHCO_3$, 100 mM HEPES buffer solution and 300 mM Taurine) to clean the tissue around the aorta under a microscope. Then the aorta was placed onto a cannula (inner diameter 1mm) with forceps and tied with silk suture to allow perfusion through the coronary arteries. Subsequently, the heart was perfused with enzyme solution containing Liberase DH (5 mg/ml, Roche, 5401089001), trypsin (1%, Gibco, 15090046) and $CaCl_2$ (100 mM) to digest the tissue at 37°C. Enzymatic digestion was ended with Stop I and II solutions containing perfusion buffer with FCS and $CaCl_2$ (10 mM). Digested heart tissue samples were passed through a 100 µm cell strainer. Then, the calcium concentration was gradually increased by manual administration to digested heart tissue with continuous gentle mixing. Then the cells were subjected to either IonOptix analysis, culturing or direct RNA and protein extraction (after cardiomyocyte sedimentation).

Isolation of Neonatal Rat Cardiomyocytes (NRCMs)

Hearts from 1-3 days old rats were collected and washed with ice-cold 1x ADS (pH 7.35) to clean the blood and remove the atria. The ventricular parts were minced in 1x ADS and digested in enzyme solution containing collagenase Type II (Worthington: LS004176) and pancreatin (Sigma P3292). The resulting cells were loaded onto a Percoll gradient to separate cardiomyocytes (NRCMs) and non-cardiomyocytes. NRCMs were seeded (4.0×10^5 /well for 6 well-plate) onto 0.5% Gelatine-coated plates.

Isolation of Extracellular Vesicles (EVs)

Isolation of EVs was performed with ultracentrifugation from the supernatant of C166 cells that were cultured with EV-depleted FCS. Initially, cell debris and large vesicles (apoptotic bodies) were removed by centrifugations at 300xg and 10.000xg, respectively. Subsequently, small EVs (including microvesicles and exosomes) were collected with 100.000xg ultracentrifugation for 90 minutes, and similarly washed with PBS, before a second round of centrifugation was performed. The EV pellet was re-suspended in PBS for NTA (ZetaView Nanoparticle Tracing Videomicroscope, PMX-120) measurements, or with QIAzol lysis buffer (Qiagen, 79306) for RNA isolation.

EV-RNA isolation. RNA isolation from EVs was performed by RNA precipitation as described before.[50] Briefly, the EV pellet was resuspended with 1 ml of QIAzol, and then mixed with 200 µl of chloroform for phase separation. Samples were mixed thoroughly and incubated for 5 minutes at room temperature (RT), then centrifuged at 12.000xg at 4°C for 15 minutes. The aqueous upper layer was mixed with 10% (v/v) sodium acetate (3M, pH 5.5) and 4 µl of glycogen (5 mg/ml) in 1.5 ml ethanol (100%). Samples were incubated at -80°C overnight, then centrifuged at 16.000xg for 30 minutes to pellet the RNA. The RNA pellet was then washed with 70% ethanol and dried, before being re-suspended in nuclease-free water.

EV RNase and Proteinase-K Protection Assay. To test the transfer of *Gadlor* lncRNAs within EVs, we performed RNase and proteinase K protection assays with and without prior the application of Triton-X. In brief, EVs were isolated and treated with 100 ng/µl of RNase A, and 20 mg/µl of proteinase K for 30 minutes at 37°C. 5 mM of PMSF was used to inactivate the proteinase K at RT. To disrupt the lipid bilayer, EVs were incubated with 1% Triton-X for 1 hour for selected samples. As a negative control, RNA isolated from EVs was also treated with the same protocol.

EV-labelling with PKH67 cell linker. To visualize EVs for transfer and re-uptake experiments *in vitro,* they were labelled with PHK67 Green Fluorescent Cell Linker kit (Sigma MIDI67). Briefly, the EV pellet was re-suspended with 1 ml of diluent C including 4 µl of PKH67 dye, and incubated for 5 minutes at RT. Then, 1% BSA-PBS was added into the suspension to remove the unspecific binding of the dye. Then EVs were pelleted at 3000xg for 1 hour, which were then suspended with the cell culture medium and added on NRCMs. Visualization of EVs was conducted with the Leica Confocal Microscope TCS SP8 and images were analyzed by Leica Application Suite X (LAS X) 3.7.

EV FACS Staining. Characterization of surface markers of EVs was performed with flow cytometry by staining EC-derived EVs with CD9-PerCP-Cy5.5 (Miltenyi Biotec, 130-102-278, Clone: MZ3), CD63-APC (Miltenyi Biotec, 130-108-894, Clone: REA563) and CD54-FITC (BD, 553252, Clone: 3E2) labelled antibodies for 1 hour at 4°C. Measurements were obtained with BD FACSCanto ll.

EV Transmission Electron Microscopy (TEM). Visualization of EVs was performed with TEM. After centrifugation, pellets were resuspended in the minimum possible volume of residual liquid and 25 % aqueous glutaraldehyde was added to a final concentration of 1 %. After fixation overnight, samples were mixed 1:1 (v/v) with 4 % agar at 40 °C. After hardening, the agar blocks were cut into cubes of 1 mm in size. Further preparation of samples and electron microscopy were performed as described, before being imaged with a FEI Morgagni 268 transmission electron microscope (FEI, Eindhoven, Netherlands) operated at 80 kV using a Veleta CCD camera (Olympus Soft Imaging Solutions).[51]

EV-mediated Gadlor1 and Gadlor2 overexpression. As a gain-of-function approach, *Gadlor1* and *Gadlor2* were overexpressed in mouse hearts by administration of *Gadlor1/2*-enriched EVs. To this end, C166 endothelial cells were infected with *Gadlor1* and *Gadlor2* adenoviruses for 48 hours. EVs were collected with ExoQuick-TC solution (EXOTC50A-1,65 SystemsBio) based on manufacturers' protocols with some adjustments. In vivo overexpression of *Gadlor* lncRNAs was achieved by injecting EVs directly into the left ventricles before TAC surgery. The intra-ventricular injection was performed by simultaneous cross-clamping of the aorta and pulmonary artery distal of the origin of the coronary vessels.

Cell Culture

C166 (CRL-2581, ATCC) mouse embryonic endothelial cells and NIH3T3 (CRL-1658, ATCC) mouse fibroblast cells were cultured in Dulbecco's Modified Eagle's Medium (DMEM) with 10% FCS, while MCECs (CLU510-P, Tebu-bio), immortalized mouse cardiac endothelial cells, were cultured with 5% FCS containing DMEM supplemented with L-glutamine (1%), penicillin/ streptomycin (1%) and HEPES. HL-1 cardiac muscle cells (SCC065, Merck) were cultured with Claycomb media (Sigma, 51800C) supplemented with 10% FCS, 0.1 mM norepinephrine, 2 mM L-glutamine and 1X penicillin-streptomycin (P/S). HL-1 cells were plated on 0.1% Gelatine-coated flasks, and cell culture media was refreshed daily. Cells were cultured for up to 10 passages.

Adenoviral infection. For overexpression of *Gadlor* lncRNAs, recombinant adenoviruses were used. Mouse cDNAs of AK037972 (*Gadlor*1) and AK038629 (*Gadlor*2) were subcloned into the pShuttleCMV vector (Source Bioscience, UK) and adenoviruses were generated by the AdEasy Adenoviral Vector system (Agilent, 240009). An adenovirus overexpressing β-Galactosidase (Adß*gal*) was used as a control. After the production of adenoviruses, the viral titer was calculated with the help of the AdEasy Viral Titer Kit (Agilent, 972500), and all the experiments were performed with 50 MOI. Adenoviral infection on cultured cells was performed for 4 hours at 37°C on cells with media containing heat-inactivated FCS.

Co-culture experiments. For co-culture experiments, adult mouse cardiomyocytes isolated from *Gadlor*-KO mice were seeded on laminin (Santa Cruz, SC-29012) coated 6-well plates and cultured with MCECs plated on 1 µm pore-sized inserts (Thincert, Greiner, 657610). Cells were collected separately after 48 hours for RNA isolation.

To inhibit EV trafficking between MCECs and CMs in the co-culture model, MCECs were pre-treated with 20 µM of GW4869 (Hoelzel Biotech) for 6 hours, and then placed for 48 hours of co-culture with isolated *Gadlor*-KO or WT CMs.

Endothelial Cell Sprouting Assay

To study the effect of *Gadlor* lncRNAs on angiogenesis, we performed sprouting assays with C166 mouse ECs according to a well-established protocol previously described.[52] Briefly, cells were infected with *Ad. ßgal or Ad.Gadlor1/2* adenovirus for 24 hours. 50.000 cells were re-suspended with 4 mL DMEM + 10 % FCS and 1 mL methylcellulose solution (Sigma-Aldrich, M0512) and drops containing 25 µl of suspension were pipetted onto a 10 cm cell culture dish. The drops were then incubated upside-down in a cell culture incubator for 24 hours to allow spheroid formation. On the following day, the cell spheroids were gently washed off the hanging drops with PBS, collected by 200xg centrifugation for 5 minutes and re-suspended with methylcellulose solution containing 20 % FCS. The collagen matrix was prepared in parallel on ice with collagen stock solution (Corning, 11563550), diluted in 10x M199 medium (Sigma-Aldrich, M0650) and the required amount of sodium hydroxide to set the pH for polymerization. Then the collagen medium was mixed with the spheroids. 1 mL of the spheroid-collagen-methylcellulose mixtures were added per well in a 24-well plate and incubated in a cell culture incubator for 30 min to induce the polymerization of the collagen-methylcellulose matrix. The endothelial spheroids were stimulated with 100 µl of DMEM + 10 % FCS, 25 ng/mL FGF2 or 10 ng/mL TGF-β1 by adding it dropwise to the collagen matrix. After 24 hours, the

sprouting assay was stopped by adding 1 mL of 4% paraformaldehyde to the wells. Spheroids were visualized with the 10X objective in bright-field microscopy and analyzed with ImageJ.

RNA Isolation and qRT-PCR

RNA isolation from tissue samples was performed with QIAzol reagent (Qiagen, 79306), and from isolated cells with NucleoSpin RNA isolation kit (Macherey-Nagel, 740955.250) according to manufacturers' protocols. Samples were incubated with rDNase (Macherey-Nagel, 740963) on the silica-columns to remove any DNA contamination. cDNA was generated by using the Maxima H minus First strand cDNA synthesis kit (Thermo Fisher Scientific, K1652). Quantitative PCR was performed with the Maxima SYBR Green mix with ROX as reference dye (Thermo Scientific, K0253) on an AriaMx Real-time PCR System (Agilent, G8830a). Gene expression was normalized to *Gapdh*,18S or *U6* expression. All qPCR primer sequences are listed in **Supplementary Table 4**.

Protein Isolation and Western blotting

Heart tissue protein lysates were prepared from frozen pulverized tissue with lysis buffer containing 30 mM Tris-pH 8.8, 5 mM EDTA-pH 8.0, 3% SDS (v/v), 10% glycerol (m/v), protease and phosphatase inhibitors. Protein quantification was performed by BCA assay (ThermoFisher, Pierce BCA Protein Assay kit, 23225). Samples were incubated at 95°C for 5 minutes after the addition of Laemmli buffer (1X final concentration) and proteins were separated with SDS-PAGE electrophoresis. The following primary antibodies were used: Calsequestrin (Thermo Scientific PA1-913, rabbit), Phospholamban, pThr17 (Badrilla A010-13, rabbit), Phospholamban (Badrilla, A010-14 mouse). The following secondary antibodies were used: Rabbit anti-mouse peroxidase (Sigma-Aldrich), and goat anti-rabbit peroxidase (Sigma-Aldrich).

Sarcomere Contractility and Calcium Transient Measurements

Adult cardiomyocytes were isolated 1-week after TAC operation. Cardiomyocytes were plated on laminin coated (10 µg/cm^2) 35 mm dishes (MatTek 10 mm Glass bottom dishes, P35G-1.5-10-C) and gently washed 1 hour later with MEM medium without butanedione monoxime (BDM). The plated cells were then transferred into the Ion-Optix Multicell High-throughput System chamber, where they were simultaneously paced (18 V, 2.5 Hz, 4 ms impulse duration), and assessed for sarcomere length and contraction. Calcium handling was recorded after incubation with 1 µM fura-2, AM (Invitrogen, F1221).

For measurements following *Gadlor1/2* overexpression via EV-mediated transfer, isolated adult cardiomyocytes were incubated with EVs for 4 hours. To assess the effect of CaMKII inhibition, cells were treated with KN93 (1 µM) for 1 hour before the measurements. The recordings were analyzed with IonWizard software.

RNA antisense purification coupled with mass spectrometry (RAP-MS)

To identify the protein interaction partners of *Gadlor* lncRNAs we performed RAP-MS as described previously with minor modifications.[53] The 5' biotinylated antisense *Gadlor1* and *Gadlor2* probes were pooled in the experiment and the sequences are listed in **Supplementary Table 5**. We used HL-1 cardiomyocytes overexpressing *Gadlor1* and *Gadlor2* after infection with Ad.*Gadlor1* and Ad.*Gadlor2.* RNA antisense purification (RAP) was performed with cells collected from five 15 cm dishes per sample, where each experimental group contained three replicates without (as a negative control to identify non-specific 'background' proteins) and four replicates with UV cross-linked conditions. HL-1 cells were washed with cold PBS twice and cross-linked using 150 mJ/cm^2 of 254 nm UV light. Cells were then lysed with lysis buffer, incubated for 10 minutes on ice, homogenized by passing several times through a 21G needle and DNA was digested with addition of DNase salt solution and Turbo DNase for 10 minutes at 37°C (ThermoFisher, AM2238). Hybridization conditions were adjusted by the addition of an equal amount of

hybridization buffer. Lysates were precleared with streptavidin-coated magnetic beads. Biotin-labelled *Gadlor1* and *Gadlor2* probes were heated to 85°C for three minutes and then incubated with the lysate for 2 hours at 67°C. Probe-RNA complexes were captured by pre-washed streptavidin-coated magnetic beads and incubated at 37°C for 30 minutes. Lysate was removed from beads by magnetic separation, and beads were washed four times in hybridization buffer at 67°C. *Gadlor* lncRNA-bound proteins were then released by Benzonase RNA digestion for two hours at 37°C. The captured protein samples were identified by TMT labelling followed by liquid chromatography-mass spectroscopy (LC-MS/MS) by the EMBL proteomics core facility.

RNA immunoprecipitation (RIP)

We performed RIP with minor modifications to a previously described protocol to confirm the interaction of *Gadlor1* and *Gadlor2* lncRNAs with CaMKII. [54] HL-1 cardiomyocytes were used to overexpress *Gadlor* lncRNAs by adenovirus treatment, while Ad.βgal treated samples were used as control. Three 15 cm plates were combined for preparation of each sample. Briefly, cells were washed with ice-cold PBS twice and lysed with polysome lysis buffer (100 mM KCl, 5 mM MgCl2, 10 mM HEPES pH 7, 0.5% IGEPAL CA-630, 0.1 mM DTT, 1 x protease inhibitor cocktail, 1 x RNasIN). Cell lysates were passed through a 26G needle multiple times for homogenization. Protein G magnetic beads (Bio-Rad SureBeads, 161-4221) were washed twice with NT-2 buffer (50 mM Tris-HCl pH 7.4, 150 mM NaCl, 5 mM MgCl2, 0.05 % IGEPAL CA-630) and coupled with anti-CaMKII antibody (Santa Cruz, sc-5306) or anti-IgG (mouse, Cell Signaling 7076, as control) overnight at 4°C. Antibody coupled beads were washed twice with NT-2 buffer and resuspended in NET-2 buffer (50 mM Tris-HCl pH 7.4, 150 mM NaCl, 5 mM MgCl2, 0.05 % IGEPAL CA-630, 20 mM EDTA pH 8, 1 mM DTT, 1 x RNaseIN). Cell lysates were added to beads and incubated at 4°C for 2 hours (10% lysate was removed as input and stored on ice prior to IP).

After supernatant was removed from the beads, 1 ml of ice-cold NT-2 buffer was used to wash the beads five times in total. Then, beads were resuspended with Proteinase K buffer (1x NT-2 buffer and 1% SDS) and incubated at 55°C for 30 minutes with constant shaking while input sample conditions were adjusted accordingly and processed in parallel. The supernatant was transferred into fresh tubes and combined with NT-2 buffer and UltraPure phenol-chloroform (ThermoFisher, 15593031) for RNA purification. After centrifugation in heavy-lock tubes at 15.000 x g for 15 minutes, RNA was purified from the clear aqueous phase with the RNA Clean and concentrator kit (Zymo Research, R1017).

RNAScope *in situ* Hybridization

In situ hybridization was performed to localize Gadlor1 (Mm-LOC118567341-C3), Gadlor2 (Mm-AK038629-C1, Cat no: 404391) and Cdh5 (Mm-Cdh5-C2, Cat no: 312531) mRNA expression on mouse heart tissue slides with RNAscope Multiplex Fluorescent v2 kit. The assay was performed according to the manufacturer's protocol. Briefly, OCT-embedded tissue slides (7 µm thickness) were used in the assay, fixed with 4% PFA and then stepwise dehydration was performed with increasing concentrations of ethanol. Tissue slides were subsequently treated with hydrogen peroxide (10 min at RT) and protease IV (30 min at RT) in the humidity control incubator. Slides were incubated for 2 hours with the mixture of probes to hybridize with the corresponding RNAs. Next, the signal was amplified with RNAScope Multiplex FL v2 AMP 1-3 reagents and then HRP channels were developed sequentially. Finally, DAPI was used to counterstain the slides and each was mounted with ProLong Gold Antifade Mountant (Fisher Scientific).

DNA Isolation and Analysis of mtDNA/ nDNA

To analyze the mitochondrial DNA (mtDNA) to nuclear DNA (nDNA) ratio of *Gadlor*-KO and WT mouse hearts after 2-weeks of TAC, genomic DNA was isolated from mouse heart tissue samples obtained after

TAC (2w) with a DNA isolation kit according to manufacturers' instructions (PureLink Genomic DNA Mini kit, Invitrogen, K182001). The mtDNA/ nDNA ratios were quantified by quantitative PCR using ND1 and 16S rRNA primers listed in **Supplementary Table 4**.

Bulk RNA sequencing and Bioinformatics

To perform RNA sequencing, RNA isolation was performed from isolated cells as described at indicated time points (2 weeks after TAC or sham surgery). Quality control of RNA samples (Agilent 2100 Fragment Analyzer), and library preparation (DNBSEQ Eukaryotic Strand-specific mRNA library) were performed by BGI, Hong Kong. Bulk RNA sequencing from different cardiac cells were performed as stranded and single-end with 50 base sequence read length by BGI with Illumina HiSeq 2500. Initially, the trimming of adapter sequences from fastq files was performed with the R package *FastqCleaner*. For aligning the reads to the reference genome (mm10) after trimming, the R package *bowtie2* alignment tool was used. Gene annotation was performed with the *bioMaRt* R package. Library size of the samples was normalized to counts per million (cpm) and transformed into log2 values followed by calculation of differential gene expression with the *edgeR* package of R. Significant changes in gene expression between compared groups were filtered based on FDR < 0.05, and fold change (FC) > 1.5. Gene ontology analysis were performed with Metascape and DAVID online tools. Heatmaps that show the differentially regulated genes were generated by heatmap.2 function in *ggplot2* library in R.

Data Availability

The authors declare that the data supporting the findings of this study are available within the paper and its supplementary information. RNA sequencing data sets were deposited in National Center for Biotechnology Information's (NCBI) Gene Expression Omnibus (GEO) repository with the accession number GSE213612.

Statistics

Data analysis and statistical analysis were performed with GraphPad Prism software (Version 8). Data are shown as mean ± standard error of the mean (SEM). All the experiments were carried out in at least 3 biological replicates. The number of replicates for animal experiments and cell culture experiments are indicated in the figure legends. The investigators were blinded for mouse genotype and treatment during surgeries, echocardiography, organ weight determination and all histological and immunofluorescence quantifications.

Initially, all the datasets were analyzed for normality to allow the application of the proper statistical test. An unpaired 2-tailed Student t-test was used for comparing 2 groups only. Comparing multiple groups for one condition was performed with one-way ANOVA and Fisher's LSD post-hoc test. Comparing multiple groups for multiple conditions was achieved with two-way ANOVA and followed with Fisher's LSD post-hoc test when applicable. For non-parametric data sets, the Mann-Whitney and Kruksal-Willis tests were used to compare two groups and multiple groups, respectively. Values of $p<0.05$ were considered statistically significant.

References

1. Tsao, C.W. *et al.* Heart Disease and Stroke Statistics-2022 Update: A Report From the American Heart Association. *Circulation* **145**, e153-e639 (2022).
2. Frantz, S., Hundertmark, M.J., Schulz-Menger, J., Bengel, F.M. & Bauersachs, J. Left ventricular remodeling post-myocardial infarction: pathophysiology, imaging, and novel therapies. *Eur Heart J* **43**, 2549-2561 (2022).
3. Wu, X., Reboll, M.R., Korf-Klingebiel, M. & Wollert, K.C. Angiogenesis after acute myocardial infarction. *Cardiovasc Res* **117**, 1257-1273 (2021).
4. Frey, N., Katus, H.A., Olson, E.N. & Hill, J.A. Hypertrophy of the heart: a new therapeutic target? *Circulation* **109**, 1580-1589 (2004).
5. Bar, C. *et al.* Non-coding RNAs: update on mechanisms and therapeutic targets from the ESC Working Groups of Myocardial Function and Cellular Biology of the Heart. *Cardiovasc Res* **116**, 1805-1819 (2020).
6. Hill, J.A. & Olson, E.N. Cardiac plasticity. *N Engl J Med* **358**, 1370-1380 (2008).
7. Heineke, J. & Molkentin, J.D. Regulation of cardiac hypertrophy by intracellular signalling pathways. *Nat Rev Mol Cell Biol* **7**, 589-600 (2006).
8. Huang, C.K., Kafert-Kasting, S. & Thum, T. Preclinical and Clinical Development of Noncoding RNA Therapeutics for Cardiovascular Disease. *Circ Res* **126**, 663-678 (2020).
9. Lu, D. & Thum, T. RNA-based diagnostic and therapeutic strategies for cardiovascular disease. *Nat Rev Cardiol* **16**, 661-674 (2019).
10. Wilusz, J.E., Sunwoo, H. & Spector, D.L. Long noncoding RNAs: functional surprises from the RNA world. *Genes Dev* **23**, 1494-1504 (2009).
11. Li, H. *et al.* lncExACT1 and DCHS2 Regulate Physiological and Pathological Cardiac Growth. *Circulation* **145**, 1218-1233 (2022).

12. Zhao, Y. *et al.* Cardiomyocyte-Specific Long Noncoding RNA Regulates Alternative Splicing of the Triadin Gene in the Heart. *Circulation* **146**, 699-714 (2022).

13. Viereck, J. *et al.* Long noncoding RNA Chast promotes cardiac remodeling. *Sci Transl Med* **8**, 326ra322 (2016).

14. Han, P. *et al.* A long noncoding RNA protects the heart from pathological hypertrophy. *Nature* **514**, 102-106 (2014).

15. Trembinski, D.J. *et al.* Aging-regulated anti-apoptotic long non-coding RNA Sarrah augments recovery from acute myocardial infarction. *Nature communications* **11**, 2039 (2020).

16. Micheletti, R. *et al.* The long noncoding RNA Wisper controls cardiac fibrosis and remodeling. *Sci Transl Med* **9** (2017).

17. Cheng, Y. *et al.* A translational study of urine miRNAs in acute myocardial infarction. *J Mol Cell Cardiol* **53**, 668-676 (2012).

18. Kuwabara, Y. *et al.* Increased microRNA-1 and microRNA-133a levels in serum of patients with cardiovascular disease indicate myocardial damage. *Circ Cardiovasc Genet* **4**, 446-454 (2011).

19. Schulte, C., Barwari, T., Joshi, A., Zeller, T. & Mayr, M. Noncoding RNAs versus Protein Biomarkers in Cardiovascular Disease. *Trends Mol Med* **26**, 583-596 (2020).

20. Heineke, J. *et al.* Cardiomyocyte GATA4 functions as a stress-responsive regulator of angiogenesis in the murine heart. *J Clin Invest* **117**, 3198-3210 (2007).

21. Sano, M. *et al.* p53-induced inhibition of Hif-1 causes cardiac dysfunction during pressure overload. *Nature* **446**, 444-448 (2007).

22. Oka, T., Akazawa, H., Naito, A.T. & Komuro, I. Angiogenesis and cardiac hypertrophy: maintenance of cardiac function and causative roles in heart failure. *Circ Res* **114**, 565-571 (2014).

23. Sluijter, J.P., Verhage, V., Deddens, J.C., van den Akker, F. & Doevendans, P.A. Microvesicles and exosomes for intracardiac communication. *Cardiovasc Res* **102**, 302-311 (2014).

1 24. Pinto, A.R. *et al.* Revisiting Cardiac Cellular Composition. *Circ Res* **118**, 400-409 (2016).
2 25. Uchida, S. & Dimmeler, S. Long noncoding RNAs in cardiovascular diseases. *Circ Res* **116**, 737-750
3 (2015).
4 26. Kenneweg, F. *et al.* Long Noncoding RNA-Enriched Vesicles Secreted by Hypoxic Cardiomyocytes
5 Drive Cardiac Fibrosis. *Mol Ther Nucleic Acids* **18**, 363-374 (2019).
6 27. Piccoli, M.T. *et al.* Inhibition of the Cardiac Fibroblast-Enriched lncRNA Meg3 Prevents Cardiac
7 Fibrosis and Diastolic Dysfunction. *Circ Res* **121**, 575-583 (2017).
8 28. Hosen, M.R. *et al.* CAD increases the long noncoding RNA PUNISHER in small extracellular
9 vesicles and regulates endothelial cell function via vesicular shuttling. *Mol Ther Nucleic Acids* **25**,
10 388-405 (2021).
11 29. Bang, C. *et al.* Cardiac fibroblast-derived microRNA passenger strand-enriched exosomes
12 mediate cardiomyocyte hypertrophy. *J Clin Invest* **124**, 2136-2146 (2014).
13 30. Hosen, M.R. *et al.* Circulating MicroRNA-122-5p Is Associated With a Lack of Improvement in Left
14 Ventricular Function After Transcatheter Aortic Valve Replacement and Regulates Viability of
15 Cardiomyocytes Through Extracellular Vesicles. *Circulation*, 101161CIRCULATIONAHA122060258
16 (2022).
17 31. Huang, G. *et al.* Identification and Comparison of Hyperglycemia-Induced Extracellular Vesicle
18 Transcriptome in Different Mouse Stem Cells. *Cells* **9** (2020).
19 32. Froese, N. *et al.* Endothelial Cell GATA2 Modulates the Cardiomyocyte Stress Response through
20 the Regulation of Two Long Non-Coding RNAs. *Biology* **11**, 1736 (2022).
21 33. Froese, N. *et al.* Analysis of myocardial cellular gene expression during pressure overload reveals
22 matrix based functional intercellular communication. *iScience* **25**, 103965 (2022).
23 34. Das, S. *et al.* Noncoding RNAs in Cardiovascular Disease: Current Knowledge, Tools and
24 Technologies for Investigation, and Future Directions: A Scientific Statement From the American
25 Heart Association. *Circ Genom Precis Med* **13**, e000062 (2020).

1 35. Dittrich, G.M. *et al.* Fibroblast GATA-4 and GATA-6 promote myocardial adaptation to pressure
2 overload by enhancing cardiac angiogenesis. *Basic Res Cardiol* **116**, 26 (2021).
3 36. Vidal, R. *et al.* Transcriptional heterogeneity of fibroblasts is a hallmark of the aging heart. *JCI*
4 *Insight* **4** (2019).
5 37. Kim, K.M., Abdelmohsen, K., Mustapic, M., Kapogiannis, D. & Gorospe, M. RNA in extracellular
6 vesicles. *Wiley Interdiscip Rev RNA* **8** (2017).
7 38. Pironti, G. *et al.* Circulating Exosomes Induced by Cardiac Pressure Overload Contain Functional
8 Angiotensin II Type 1 Receptors. *Circulation* **131**, 2120-2130 (2015).
9 39. Mattiazzi, A. *et al.* Chasing cardiac physiology and pathology down the CaMKII cascade. *Am J*
10 *Physiol Heart Circ Physiol* **308**, H1177-1191 (2015).
11 40. Kirchhefer, U., Schmitz, W., Scholz, H. & Neumann, J. Activity of cAMP-dependent protein kinase
12 and Ca2+/calmodulin-dependent protein kinase in failing and nonfailing human hearts.
13 *Cardiovasc Res* **42**, 254-261 (1999).
14 41. Backs, J. *et al.* The delta isoform of CaM kinase II is required for pathological cardiac hypertrophy
15 and remodeling after pressure overload. *Proc Natl Acad Sci U S A* **106**, 2342-2347 (2009).
16 42. Li, C. *et al.* The deltaA isoform of calmodulin kinase II mediates pathological cardiac hypertrophy
17 by interfering with the HDAC4-MEF2 signaling pathway. *Biochem Biophys Res Commun* **409**, 125-
18 130 (2011).
19 43. Beckendorf, J., van den Hoogenhof, M.M.G. & Backs, J. Physiological and unappreciated roles of
20 CaMKII in the heart. *Basic Res Cardiol* **113**, 29 (2018).
21 44. Mattiazzi, A. & Kranias, E.G. The role of CaMKII regulation of phospholamban activity in heart
22 disease. *Front Pharmacol* **5**, 5 (2014).
23 45. Kemi, O.J. *et al.* Aerobic interval training enhances cardiomyocyte contractility and Ca2+ cycling
24 by phosphorylation of CaMKII and Thr-17 of phospholamban. *J Mol Cell Cardiol* **43**, 354-361
25 (2007).

46. Gonzalez-Teran, B. *et al.* Transcription factor protein interactomes reveal genetic determinants in heart disease. *Cell* **185**, 794-814 e730 (2022).

47. Haq, S. *et al.* Differential activation of signal transduction pathways in human hearts with hypertrophy versus advanced heart failure. *Circulation* **103**, 670-677 (2001).

48. George, S.H. *et al.* Developmental and adult phenotyping directly from mutant embryonic stem cells. *Proc Natl Acad Sci U S A* **104**, 4455-4460 (2007).

49. Louch, W.E., Sheehan, K.A. & Wolska, B.M. Methods in cardiomyocyte isolation, culture, and gene transfer. *J Mol Cell Cardiol* **51**, 288-298 (2011).

50. Prendergast, E.N. *et al.* Optimizing exosomal RNA isolation for RNA-Seq analyzes of archival sera specimens. *PLoS One* **13**, e0196913 (2018).

51. Grund, A. *et al.* TIP30 counteracts cardiac hypertrophy and failure by inhibiting translational elongation. *EMBO molecular medicine* **11**, e10018 (2019).

52. Tetzlaff, F. & Fischer, A. Human Endothelial Cell Spheroid-based Sprouting Angiogenesis Assay in Collagen. *Bio Protoc* **8**, e2995 (2018).

53. McHugh, C.A. & Guttman, M. RAP-MS: A Method to Identify Proteins that Interact Directly with a Specific RNA Molecule in Cells. *Methods Mol Biol* **1649**, 473-488 (2018).

54. Gagliardi, M. & Matarazzo, M.R. RIP: RNA Immunoprecipitation. *Methods Mol Biol* **1480**, 73-86 (2016).

Acknowledgements

This study was supported by grants from SFB1366 (CRC1366 - Vascular Control of Organ Function)/ 1-A6 (J.H.) by the Deutsche Forschungsgemeinschaft (DFG). The authors thank the Core Facilities Pre-Clinical

Models, Live Cell Imaging Mannheim (LIMA) and the Transgenic Mice Service Unit (TGSM) at Helmholtz Centre for Infection Research (HZI) for generating the knockout mice. The authors also acknowledge EMBL Proteomics Core Facility for performing proteomics analysis.

Author contributions

M.K designed and performed the experiments, analyzed RNAseq data and wrote the first draft of the manuscript. **S.G** designed and performed the experiments and analyzed data. **N.F**, **F.A.T**, **R.W**, **S.H, S.L, G.M.D, M.S** and **R.H** performed experiments. **D.W** designed and supervised the generation of *Gadlor*-KO mice. **N.W** maintained the mouse colonies and performed experiments. **P.-S. K., Ja.H, D.F, S.U, K.B, A.M.G** and **J.C** provided experimental support for the study. **No.F., J.B., G.D.** and **T. W.** provide crucial advice for the study and critically revised the paper. **J.H.** designed and conceptualized the study, supervised all the experiments, and prepared the final draft of the manuscript. All authors read and approved the manuscript.

Competing Interest

The following patent has been granted to N.F., J.B. and J.H.: LncRNAs Gadlor1 and Gadlor2 for use in treating and preventing cardiac remodeling. US11208656 (granted 28.01.2021). The other authors declare that not no conflict of interest exists.

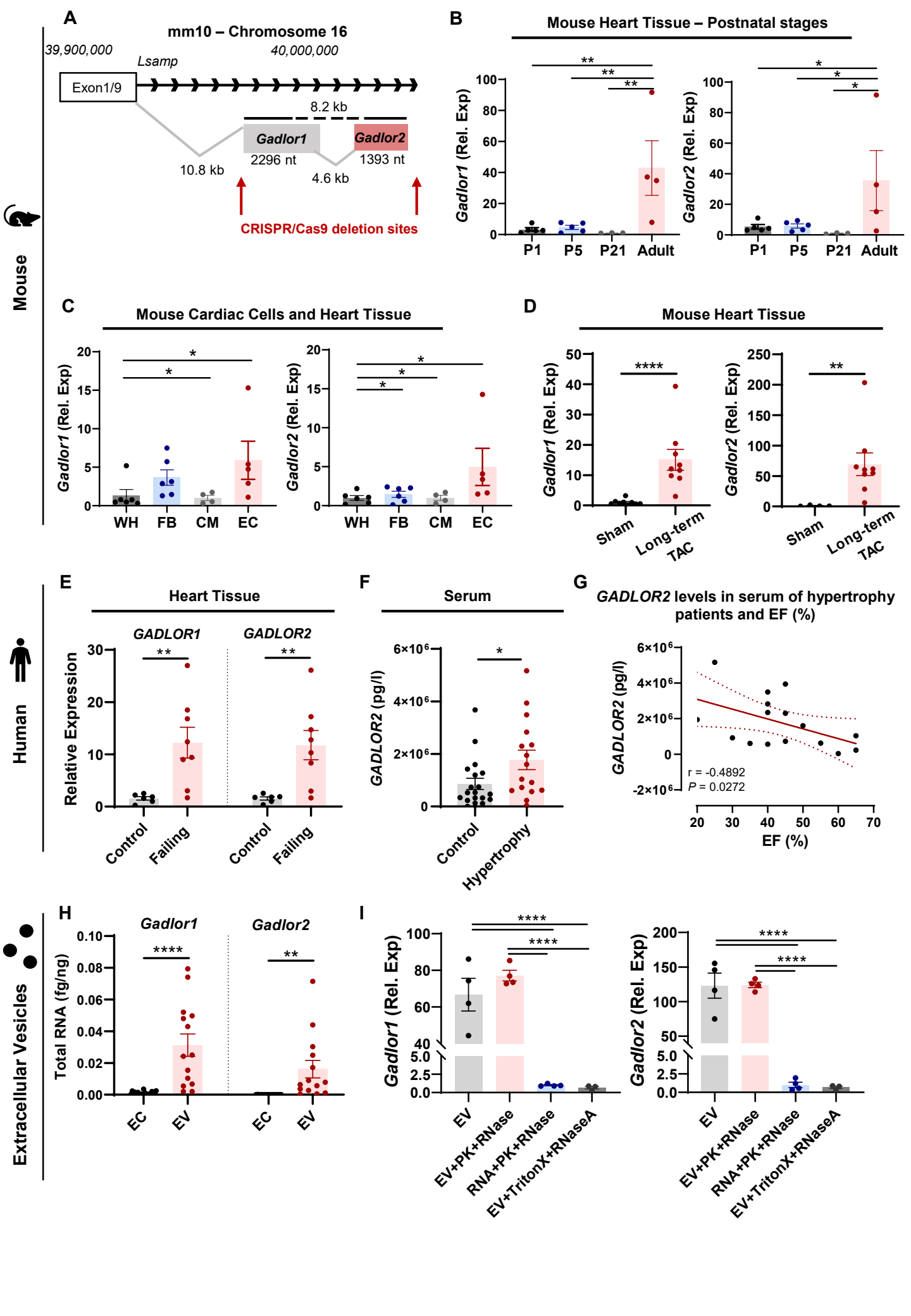
A
mm10 – Chromosome 16
39,900,000
40,000,000
Lsamp
Exon1/9
8.2 kb
Gadlor1
Gadlor2
2296 nt
1393 nt
10.8 kb
4.6 kb
CRISPR/Cas9 deletion sites
B
Mouse Heart Tissue – Postnatal stages
Gadlor1 (Rel. Exp)
Gadlor2 (Rel. Exp)
P1
P5
P21
Adult
C
Mouse Cardiac Cells and Heart Tissue
WH
FB
CM
EC
D
Mouse Heart Tissue
Sham
Long-term TAC
Mouse
E
Heart Tissue
GADLOR1
GADLOR2
Relative Expression
Control
Failing
F
Serum
GADLOR2 (pg/l)
Control
Hypertrophy
G
GADLOR2 levels in serum of hypertrophy patients and EF (%)
r = -0.4892
P = 0.0272
EF (%)
Human
H
Gadlor1
Gadlor2
Total RNA (fg/ng)
EC
EV
I
EV
EV+PK+RNase
RNA+PK+RNase
EV+TritonX+RNaseA
Extracellular Vesicles

Figure 1: *Gadlor* lncRNAs *are* mainly expressed in cardiac endothelial cells (ECs) and their expression is highly increased in mice after pressure-overload and in human failing hearts.

A. Representative scheme of AK037972 *(Gadlor1)* and AK038629 *(Gadlor2)* locus on mouse chromosome 16 and positions of the CRISPR/ Cas9 deletion sites used to generate *Gadlor*-KO mouse line. **B.** *Gadlor1* and *Gadlor2* expression levels in mouse cardiac tissue from different post-natal developmental stages (P1 – n=5, P5 – n= 5, P21 – n=3 and adult (9-weeks old) – n=4), and in **C.** different cardiac cell-types (EC: endothelial cells – n=5, FB: fibroblast – n=6, CM: cardiomyocytes – n=4) and heart tissue (WH: whole heart – n=6). **D.** *Gadlor* lncRNA levels in mouse cardiac tissue after long-term (12 weeks, n=9) TAC (transverse aortic constriction) compared to sham. **E.** *GADLOR1* and *2* expression in control (healthy, n=6) and human failing heart tissue (n=8) samples that were obtained from aortic stenosis patients. **F.** Detection of *GADLOR2* levels (pg/l: picogram/liter) in human serum of healthy volunteers (n=19) and patients with aortic stenosis (n=16). **G.** Correlation analysis of *GADLOR2* levels (pg/l) with ejection fraction (%) of hypertrophy patients (n=16), (Pearson correlation, Pearson r= -4892 and p-value = 0.0272). **H.** Absolute quantification of total RNA amount of *Gadlor1* and *Gadlor2* in ECs and EC-derived EVs (fg/ng: femtogram/ nanogram). **I.** Detection of *Gadlor* lncRNAs in EC-derived EVs with proteinase K (PK), RNase or Triton-X as indicated. Data are shown as mean±SEM. Data normality was evaluated with the Shapiro-Wilk test. *P*-values were calculated with Student's t-test for parametric (or Mann-Whitney for non-parametric) for comparing two groups, and one-way ANOVA was applied for comparing multiple groups followed with Fisher's LSD post-hoc test. *p-value<0.05, **p-value<0.01, ***p-value<0.001, ****p-value<0.0001.

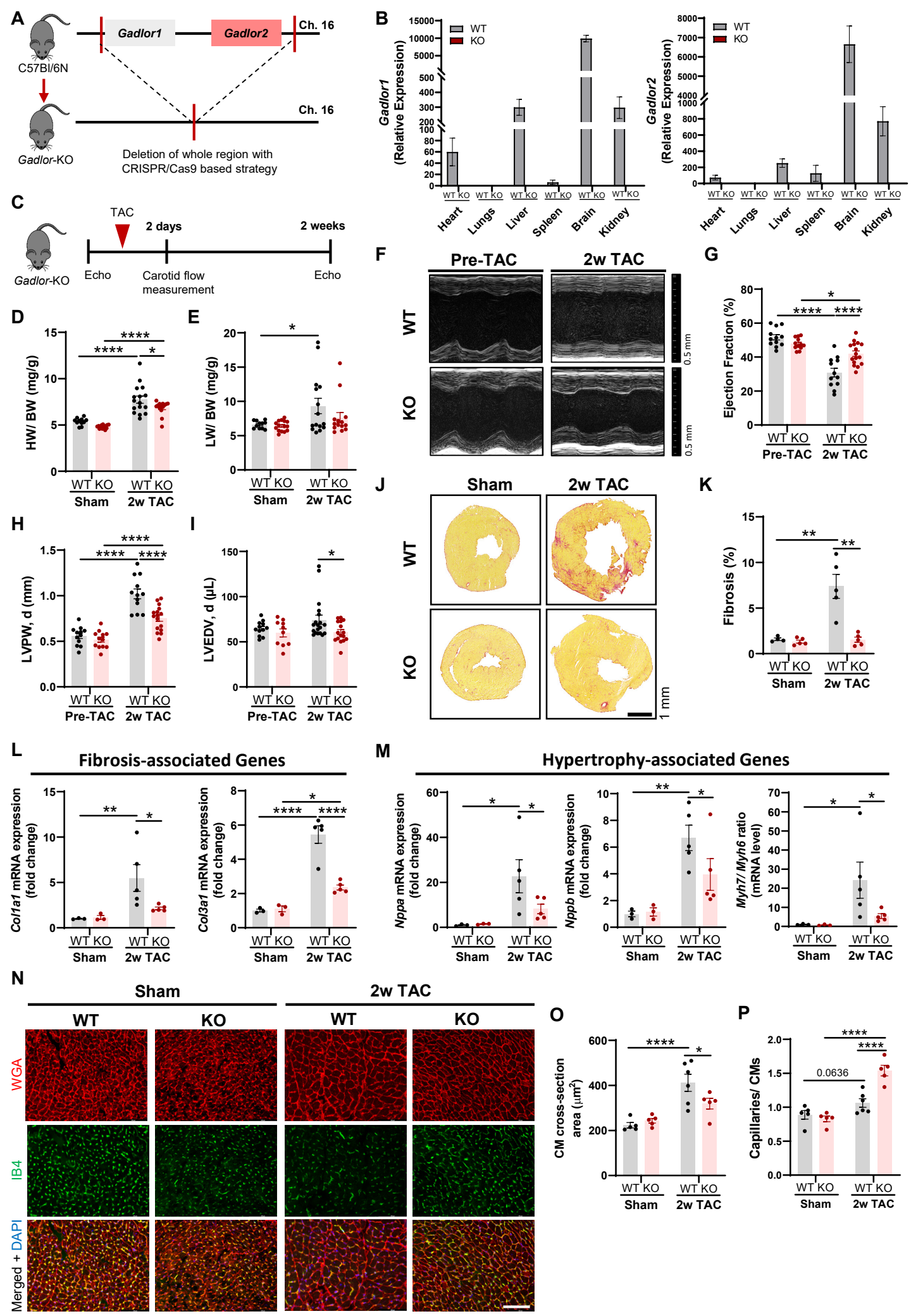
A
C57Bl/6N
Gadlor1
Gadlor2
Ch. 16
Ch. 16
Gadlor-KO
Deletion of whole region with CRISPR/Cas9 based strategy
B
WT
KO
Gadlor1 (Relative Expression)
Gadlor2 (Relative Expression)
Heart
Lungs
Liver
Spleen
Brain
Kidney
C
TAC
2 days
2 weeks
Gadlor-KO
Echo
Carotid flow measurement
Echo
D
HW/ BW (mg/g)
E
LW/ BW (mg/g)
Sham
2w TAC
F
Pre-TAC
2w TAC
WT
KO
0.5 mm
G
Ejection Fraction (%)
Pre-TAC
2w TAC
H
LVPW, d (mm)
I
LVEDV, d (µL)
J
Sham
2w TAC
1 mm
K
Fibrosis (%)
L
Fibrosis-associated Genes
Col1a1 mRNA expression (fold change)
Col3a1 mRNA expression (fold change)
M
Hypertrophy-associated Genes
Nppa mRNA expression (fold change)
Nppb mRNA expression (fold change)
Myh7/ Myh6 ratio (mRNA level)
N
Sham
2w TAC
WT
KO
WGA
IB4
Merged + DAPI
O
CM cross-section area (µm²)
P
Capillaries/ CMs
0.0636

Figure 2: Deletion of *Gadlor* lncRNAs reduces cardiac hypertrophy and fibrosis after cardiac pressure overload.

A. Scheme of *Gadlor*-KO mouse line generation by systemic deletion of the region on chromosome 16 containing both *Gadlor1* and *Gadlor2* by a CRISPR/Cas9 approach. **B.** Validation of *Gadlor*-KO mouse line by assessing the relative expression of *Gadlor*s in indicated organs in adult WT and *Gadlor*-KO mice (n≥8). The difference in *Gadlor1/2* expression levels between WT and *Gadlor*-KO animals were significant for all organs in which *Gadlor1* and *Gadlor2* were detected. (Heart: *p-value<0.05, Liver and Kidney: ***p-value<0.001, Brain: ****p-value<0.0001). **C.** Experimental design of TAC operation for *Gadlor*-KO and WT littermates. **D.** Heart weight (miligrams) to body weight (grams) ratio (HW/BW) and **E.** lung weight (miligrams) to body weight (grams) ratio of *Gadlor*-KO and WT littermates in sham and after 2 weeks TAC (n≥11). **F.** Representative echocardiography images of *Gadlor*-KO and WT mice before (pre-TAC) and after 2 weeks of TAC (2w TAC) shown in parasternal long axis mode, and analysis of **G.** left ventricle (LV) ejection fraction (EF%), **H.** LV posterior wall thickness in diastole (mm) and **I.** LV end diastolic volume (ul), (n≥12). **J.** Representative Sirius-red fibrosis staining in cardiac tissue sections of sham and 2w TAC animals (scale-bar: 1 mm) and **K.** quantification of fibrotic area (n≥4). **L.** Relative expression of fibrosis marker genes *Col1a1* and *Col3a1* and **M.** hypertrophy marker genes *Nppa, Nppb* and *Mhy7/6* ratio in mRNA levels in heart tissue samples of sham (n=3) and 2w TAC (n=5). **N.** Representative immunofluorescence images of cardiac tissue samples stained with WGA (wheat-germ agglutinin coupled with Alexa Fluor 555) and IB4 (Isolectin B4 coupled with Alexa Fluor 488) in sham and 2-week TAC samples from *Gadlor*-KO and WT littermates, scale-bar: 100 µm. Quantification of **O.** cardiomyocyte cross-sectional area and **P.** myocardial capillary density per cardiomyocyte ratio. Data are shown as mean±SEM. Data normality was evaluated with Shapiro-Wilk test and p-values were calculated with Student's t-test for comparing two groups and two-way ANOVA for grouped analysis followed with Fisher's LSD post-hoc test. *p-value<0.05, **p-value<0.01, ***p-value<0.001, ****p-value<0.0001.

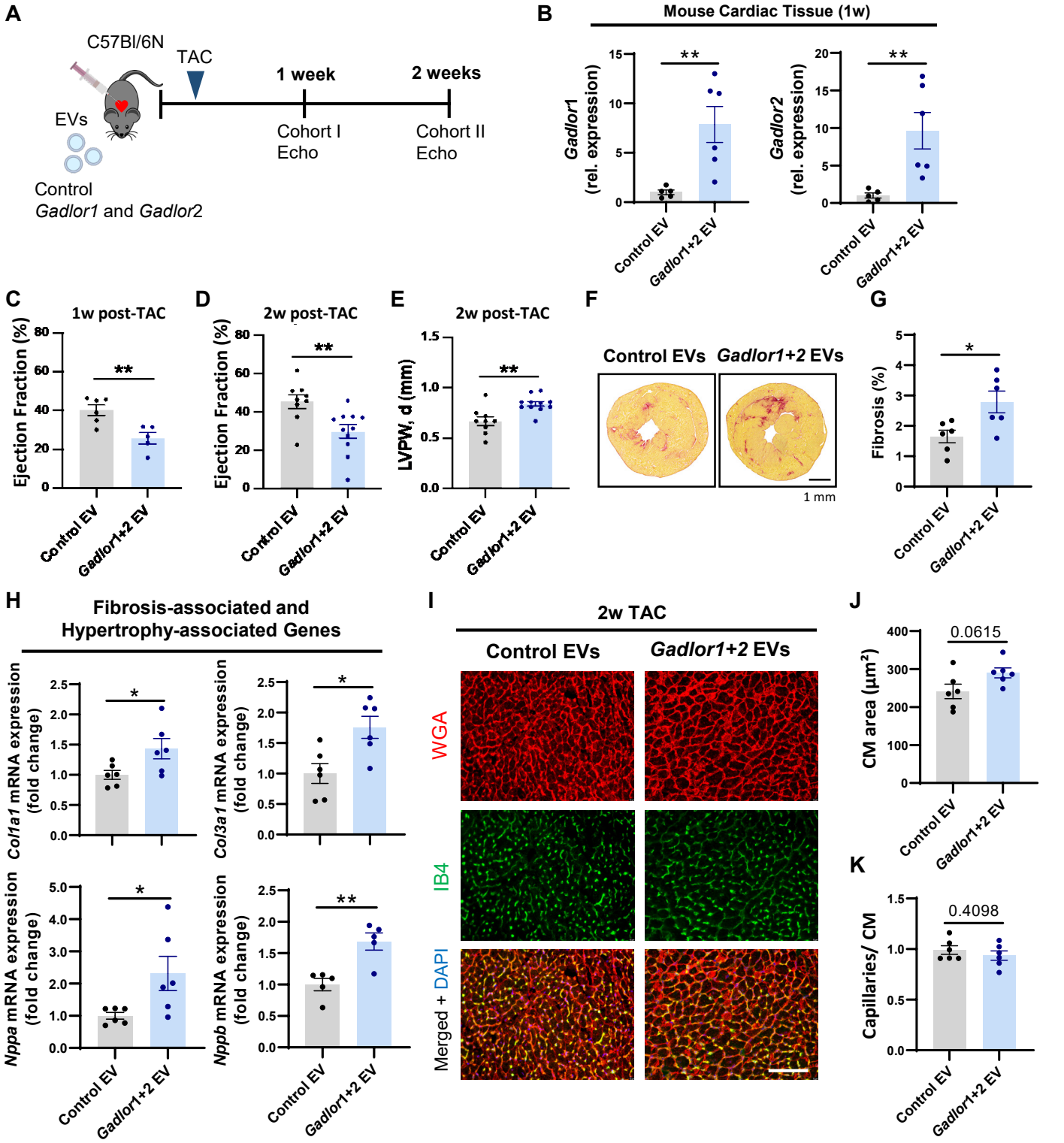

Figure 3: Overexpression of *Gadlor1* and *Gadlor2* via extracellular vesicles triggers cardiac dysfunction and development of fibrosis after TAC.

A. Scheme of the experimental design depicting the injection of *Gadlor1 and Gadlor2* containing extracellular vesicles for overexpression followed by TAC operation. **B.** Relative expression of *Gadlor1 and Gadlor2* in cardiac tissue samples after 1 week TAC (indicated as cohort I) to validate the overexpression after injection of control (Ad.βgal treated samples, n=5) and *Gadlor*-containing (Ad.*Gadlor1* and Ad.*Gadlor2* treated samples, n=6) EVs. Echocardiographic analysis of **C.** left ventricle (LV) ejection fraction (EF%) after 1 week TAC, and **D.** LV-EF%, **E.** LV posterior wall thickness in diastole (mm) after 2 weeks TAC in mice injected with control EVs and *Gadlor*1 and *Gadlor2* EVs. **F.** Representative images of Sirius-red staining (scale bar: 1 mm) and **G.** quantification of fibrotic area after 2 weeks TAC in mice injected with control EVs and *Gadlor*1 and *2* EVs. **H.** Relative expression of fibrosis marker genes *Col1a1* and *Col3a1* and hypertrophy marker genes *Nppa* and *Nppb* in heart tissue samples of control EV (n=6) and *Gadlor* EVs (n=6) treated mice. **I.** Representative immunofluorescence images of cardiac tissue samples stained with WGA (wheat-germ agglutinin coupled with Alexa Fluor 555) and IB4 (Isolectin B4 coupled with Alexa Fluor 488) in samples from control-EV and *Gadlor*-EV treated animals (scale-bar: 100 µm). Quantification of **J.** cardiomyocyte cross-sectional area and **K.** myocardial capillarization after EV treatment followed by 2 weeks of TAC. Data are shown as mean±SEM. Data normality was evaluated with Shapiro-Wilk test and p-values were calculated with Student's t-test. *p-value<0.05, **p-value<0.01, ***p-value<0.001, ****p-value<0.0001.

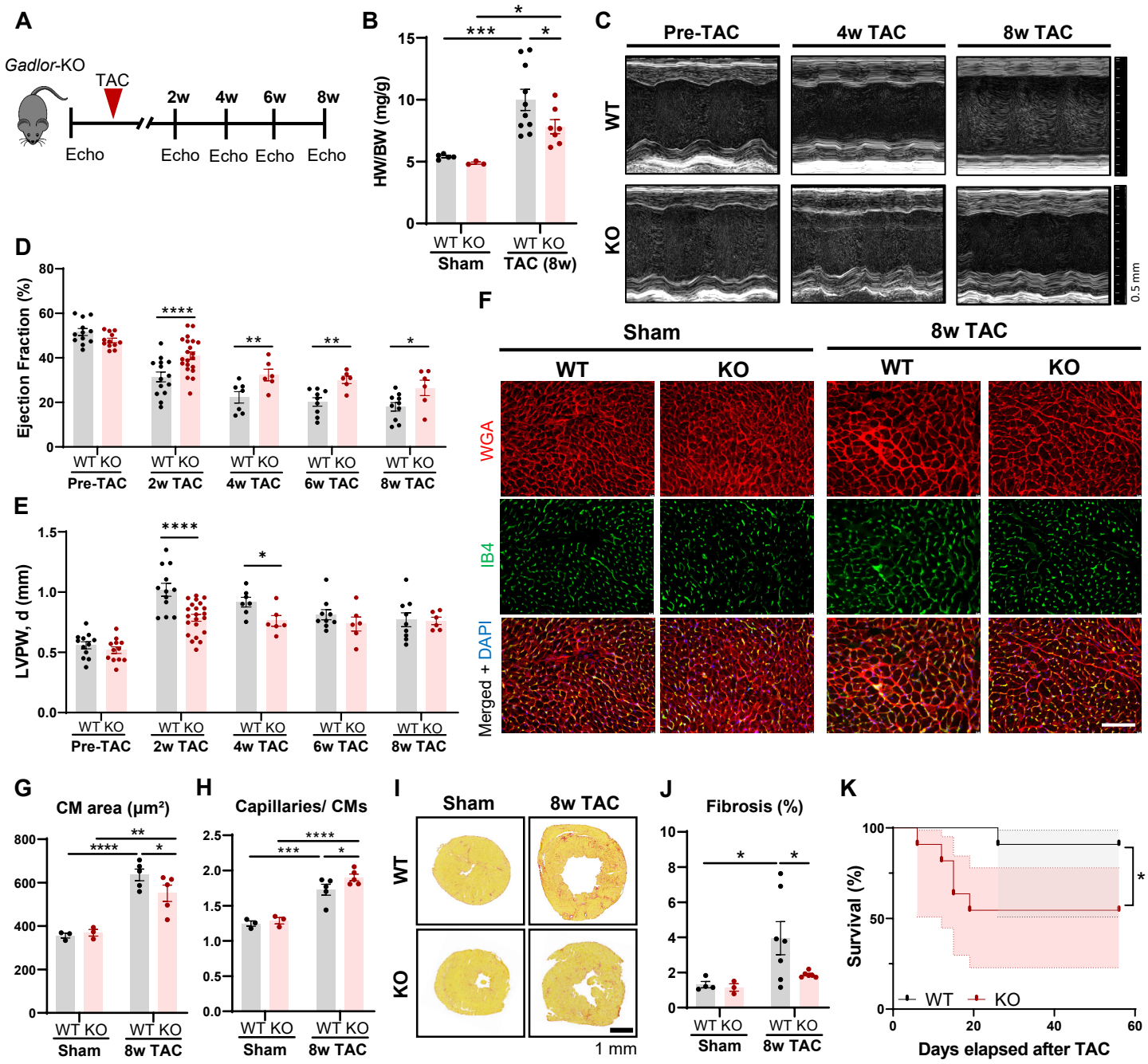

Figure 4: *Gadlor*-KO mice showed higher mortality despite retaining better structural and physiological remodeling after persisting pressure-overload.

A. Experimental design of long-term TAC operation for *Gadlor*-KO and WT littermates up to 8-weeks after TAC. **B.** Heart weight (mg) to body weight (g) ratio (HW/BW) of *Gadlor*-KO and WT mice in age comparable sham (n≥3) and after 8-weeks TAC (n≥7). **C.** Representative echocardiography images of *Gadlor*-KO and WT mice before (pre-TAC) and after 4-weeks and 8-weels TAC shown in parasternal long axis mode, and analysis of **D.** left ventricle (LV) ejection fraction (EF%) and **E.** left ventricle (LV) posterior wall thickness in diastole (mm), (unpaired analysis)**. F.** Representative immunofluorescence images of cardiac tissue samples stained with WGA (wheat-germ agglutinin coupled with Alexa Fluor 555) and IB4 (Isolectin B4 coupled with Alexa Fluor 488) in sham (n=3) and 8-week TAC (n=5) samples from *Gadlor*-KO and WT littermates, scale-bar: 100 µm. Quantification of **G.** cardiomyocyte cross-sectional area and **H.** myocardial capillary density per cardiomyocyte ratio. **I.** Representative Sirius-red fibrosis staining in cardiac tissue sections of sham (n≥3) and 8-week TAC (n≥6) mice (scale-bar: 1 mm) and **J.** quantification of fibrotic area (%). **K.** Survival of *Gadlor*-KO and WT mice after TAC (n=11). Probability of survival compared with log-rank (Mantel-Cox) test. Data are shown as mean±SEM. Data normality was evaluated with Shapiro-Wilk test and p-values were calculated with Student's t-test for comparing two groups and two-way ANOVA for grouped analysis followed with Fisher's LSD post-hoc test. *p-value<0.05, **p-value<0.01, ***p-value<0.001, ****p-value<0.0001.

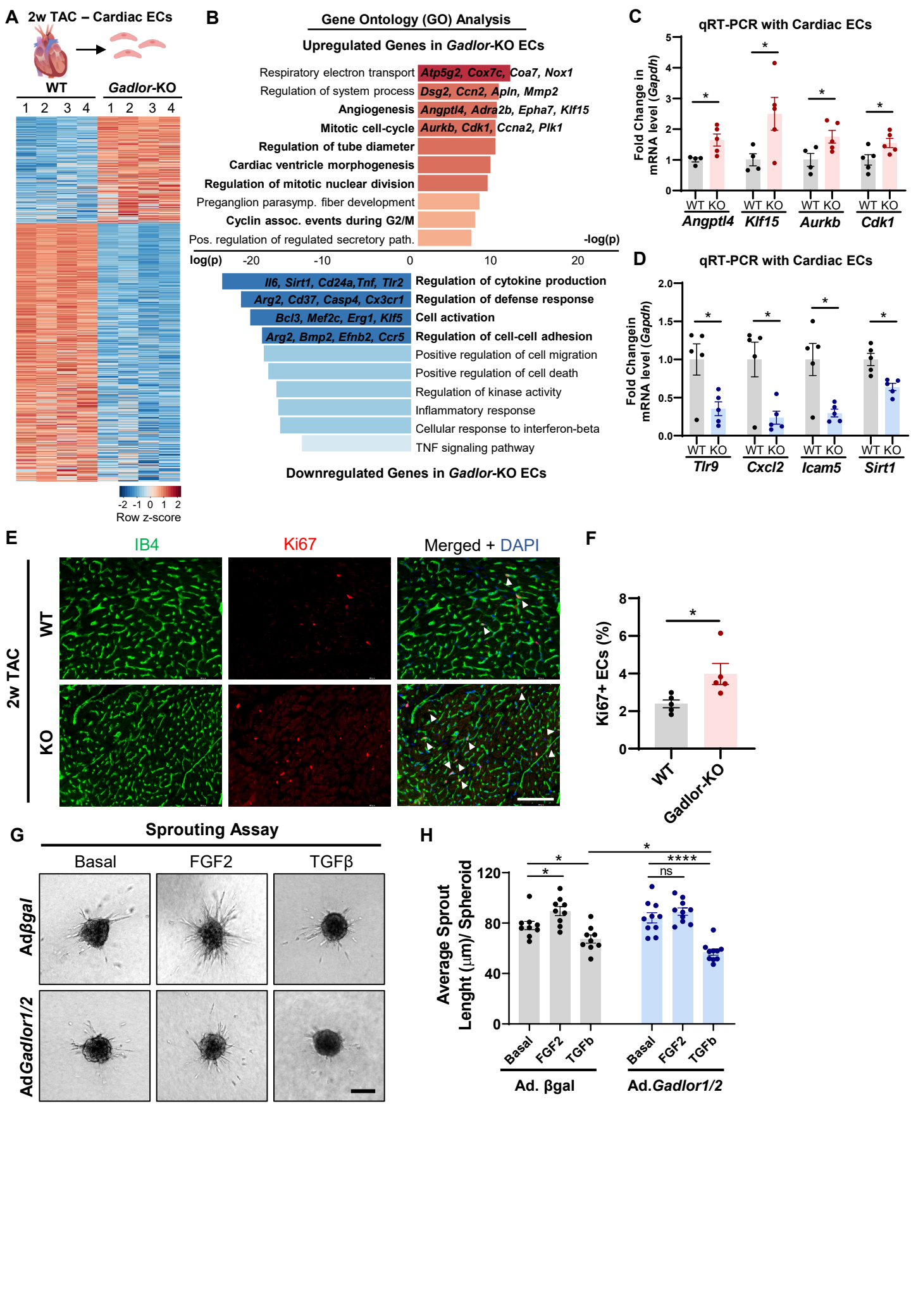
A
2w TAC – Cardiac ECs
WT
Gadlor-KO
1 2 3 4
1 2 3 4
-2 -1 0 1 2
Row z-score
B
Gene Ontology (GO) Analysis
Upregulated Genes in Gadlor-KO ECs
Respiratory electron transport
Atp5g2, Cox7c, Coa7, Nox1
Regulation of system process
Dsg2, Ccn2, Apln, Mmp2
Angiogenesis
Angptl4, Adra2b, Epha7, Klf15
Mitotic cell-cycle
Aurkb, Cdk1, Ccna2, Plk1
Regulation of tube diameter
Cardiac ventricle morphogenesis
Regulation of mitotic nuclear division
Preganglion parasymp. fiber development
Cyclin assoc. events during G2/M
Pos. regulation of regulated secretory path.
-log(p)
log(p) -20 -10 0 10 20
Il6, Sirt1, Cd24a,Tnf, Tlr2
Regulation of cytokine production
Arg2, Cd37, Casp4, Cx3cr1
Regulation of defense response
Bcl3, Mef2c, Erg1, Klf5
Cell activation
Arg2, Bmp2, Efnb2, Ccr5
Regulation of cell-cell adhesion
Positive regulation of cell migration
Positive regulation of cell death
Regulation of kinase activity
Inflammatory response
Cellular response to interferon-beta
TNF signaling pathway
Downregulated Genes in Gadlor-KO ECs
C
qRT-PCR with Cardiac ECs
Fold Change in mRNA level (Gapdh)
WT KO
Angptl4
Klf15
Aurkb
Cdk1
D
qRT-PCR with Cardiac ECs
Fold Changein mRNA level (Gapdh)
Tlr9
Cxcl2
Icam5
Sirt1
E
IB4
Ki67
Merged + DAPI
2w TAC
WT
KO
F
Ki67+ ECs (%)
WT
Gadlor-KO
G
Sprouting Assay
Basal
FGF2
TGFβ
Adβgal
AdGadlor1/2
H
Average Sprout Lenght (μm)/ Spheroid
Basal
FGF2
TGFb
Ad. βgal
Ad.Gadlor1/2
ns
****

Figure 5: Deletion of *Gadlor* lncRNAs induces angiogenesis and expression of cell cycle genes in cardiac ECs during pressure-overload.

A. Heatmap showing differentially regulated genes revealed by bulk RNAseq of cardiac endothelial-cells after 2-weeks TAC. **B.** Bar plots showing the gene-ontology (GO) analysis of upregulated and downregulated genes in *Gadlor*-KO ECs compared to WT ECs after 2-weeks TAC (Red: Upregulated in *Gadlor*-KO, Blue: Downregulated in *Gadlor*-KO). Some exemplary genes were listed for selected GO-terms. **C-D.** Validation of selected genes from RNAseq data with qRT-PCR in isolated cardiac ECs after 2 weeks of TAC (Red: Upregulated in *Gadlor*-KO, Blue: Downregulated in *Gadlor*-KO). **E.** Representative immunofluorescence images of cardiac tissue samples stained with IB4 (Isolectin B4 coupled with Alexa Fluor 488) and Ki67 (coupled with Alexa Fluor 555) in 2-week TAC samples from *Gadlor*-KO and WT littermates, Scale bar: 100 µm. (Arrows showing Ki67+ ECs) **F.** Quantification of Ki67 positive endothelial-cells percentage (Ki67+ ECs%). **G.** Representative images of sprouting assay with C166 mouse ECs after adenovirus treatment (Ad*βgal* and Ad*Gadlor1/2*) followed by 24-hour FGF2 or TGFβ treatment. 3-dimentional (3D) collagen matrix embedded spheroids were allowed to form sprouts for 24 hours. Scale bar: 100 µm. **H.** Quantification of average sprout length per spheroid. Data are shown as mean±SEM. Data normality was evaluated with Shapiro-Wilk test. P-values were calculated with Student's t-test for comparing two groups. For grouped analysis, p-values were evaluated with two-way ANOVA followed with Fisher's LSD post-doc test. *p-value<0.05, **p-value<0.01, ***p-value<0.001, ****p-value<0.0001.

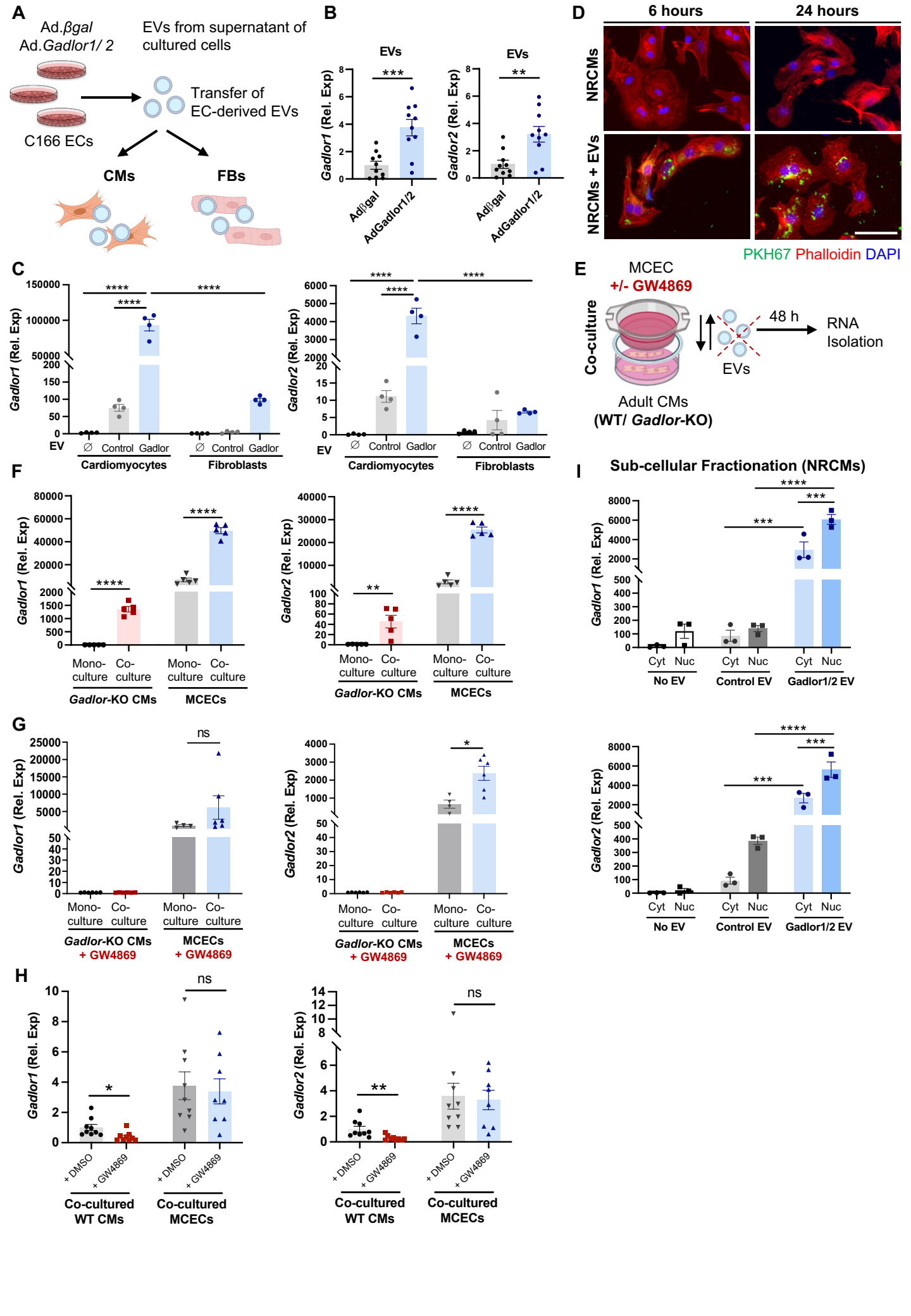
A
Ad.βgal
Ad.Gadlor1/ 2
EVs from supernatant of cultured cells
C166 ECs
Transfer of EC-derived EVs
CMs
FBs
B
EVs
Gadlor1 (Rel. Exp)
Gadlor2 (Rel. Exp)
Adβgal
AdGadlor1/2
D
6 hours
24 hours
NRCMs
NRCMs + EVs
PKH67 Phalloidin DAPI
C
Gadlor1 (Rel. Exp)
Gadlor2 (Rel. Exp)
EV
Control
Gadlor
Cardiomyocytes
Fibroblasts
E
MCEC
+/- GW4869
Co-culture
48 h
RNA Isolation
EVs
Adult CMs
(WT/ Gadlor-KO)
F
Gadlor1 (Rel. Exp)
Gadlor2 (Rel. Exp)
Mono-culture
Co-culture
Gadlor-KO CMs
MCECs
I
Sub-cellular Fractionation (NRCMs)
Gadlor1 (Rel. Exp)
Gadlor2 (Rel. Exp)
Cyt
Nuc
No EV
Control EV
Gadlor1/2 EV
G
Gadlor1 (Rel. Exp)
Gadlor2 (Rel. Exp)
Mono-culture
Co-culture
Gadlor-KO CMs + GW4869
MCECs + GW4869
H
Gadlor1 (Rel. Exp)
Gadlor2 (Rel. Exp)
+ DMSO
+ GW4869
Co-cultured WT CMs
Co-cultured MCECs

Figure 6: Secreted *Gadlor* lncRNAs are transferred to cardiomyocytes via endothelial-derived EVs.

A. Schematic representation of experimental design of EV (isolated from C166 endothelial cells, EC, supernatant) transfer to NRCMs or NRFBs. **B.** Validation of *Gadlor1* and *Gadlor2* overexpression in isolated EVs. **C.** RT-qPCR detection of *Gadlor1* and *Gadlor2* after transferring control EVs (isolated from Adβgal treated ECs) or Gadlor-EVs (isolated from Ad*Gadlor1/2* treated ECs) on neonatal rat cardiomyocytes (NRCMs) or neonatal rat cardiac fibroblasts (NRFBs). The samples were collected after 6 hours of EV incubation. **D.** Visualization of NRCMs that were incubated with PKH67-labelled (green) EVs isolated from C166 ECs for 6 hours and 24 hours. Staining was performed with Phalloidin (red) and DAPI (blue). Scale bar: 50 µm. **E.** Scheme of co-culture experiment with transwell (1 µm pore diameter – allows EV transfer). Mouse WT cardiac EC (MCEC) on top cultured with *Gadlor*-KO or WT CMs in the bottom well without direct cell contact. **F.** RT-qPCR detection of *Gadlor1* and *Gadlor2* in isolated *Gadlor*-KO CMs and MCEC mouse ECs after 48 hours of mono-culture or co-culture as indicated. **G-H.** RT-qPCR detection of *Gadlor1* and *Gadlor2* in isolated adult *Gadlor*-KO CMs (G) or WT CMs (H) and MCECs that were incubated with GW4869 as indicated. Samples were collected after 48 hours of mono-culture and co-culture. DMSO was used as vehicle control. **I.** *Gadlor1* and *Gadlor2* expression in the cytosol and nucleus of the recipient NRCMs after EV transfer (as shown in A). Data are shown as mean±SEM. Data normality was evaluated with Shapiro-Wilk test and p-values were calculated with Student's t-test or one-way ANOVA with Fisher's LSD post-hoc test were applied for comparing two or multiple groups, respectively. Two-way ANOVA with Fisher's LSD post-hoc test was applied for grouped analysis when applicable. *p-value<0.05, **p-value<0.01, ***p-value<0.001, ****p-value<0.0001.

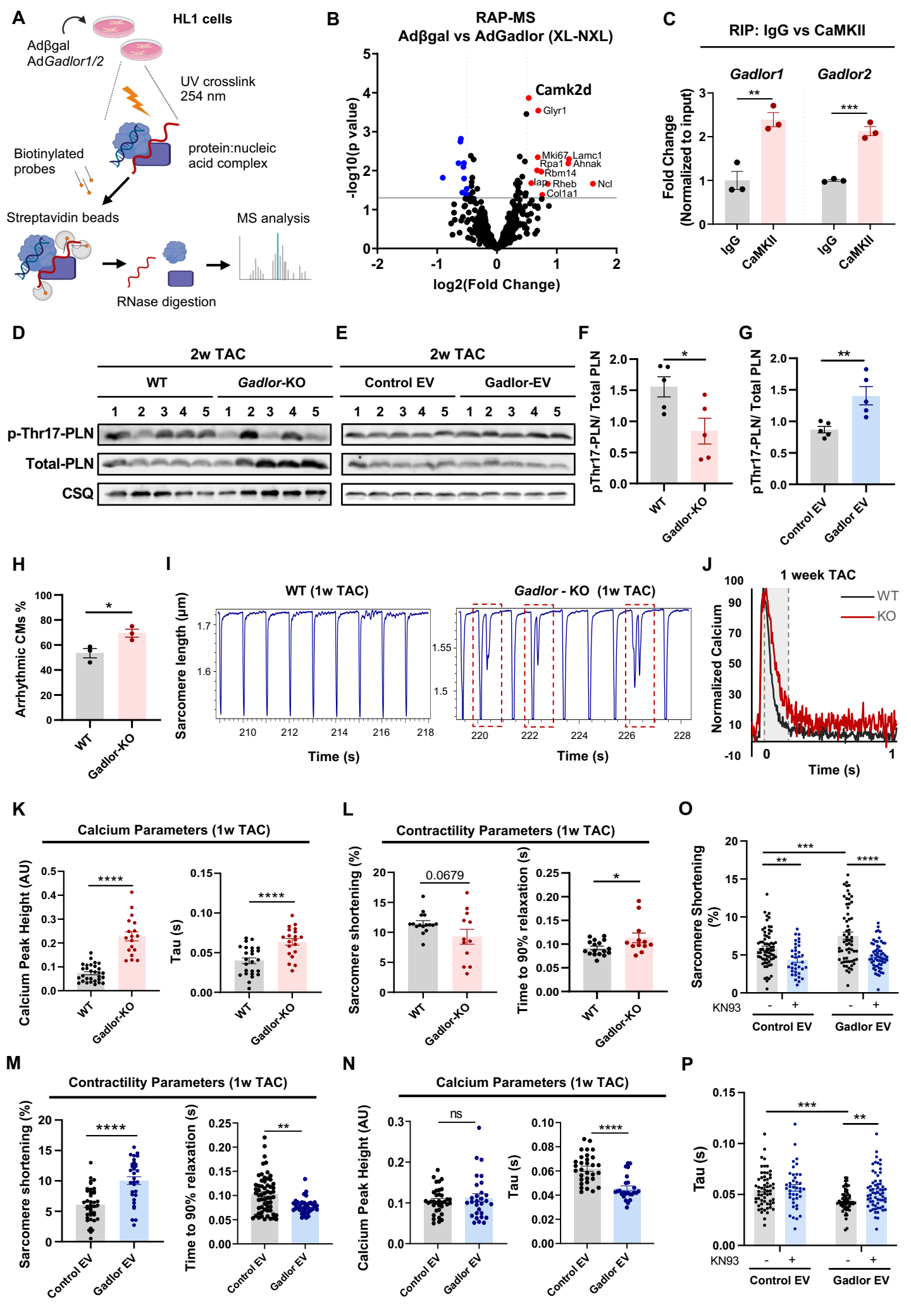
A
HL1 cells
Adβgal
AdGadlor1/2
UV crosslink
254 nm
Biotinylated
probes
protein:nucleic
acid complex
Streptavidin beads
MS analysis
RNase digestion
B
RAP-MS
Adβgal vs AdGadlor (XL-NXL)
Camk2d
Glyr1
Mki67
Lamc1
Rpa1
Ahnak
Rbm14
Iap
Rheb
Ncl
Col1a1
-log10(p value)
log2(Fold Change)
C
RIP: IgG vs CaMKII
Gadlor1
Gadlor2
Fold Change
(Normalized to input)
IgG
CaMKII
D
2w TAC
WT
Gadlor-KO
p-Thr17-PLN
Total-PLN
CSQ
E
2w TAC
Control EV
Gadlor-EV
F
pThr17-PLN/ Total PLN
WT
Gadlor-KO
G
pThr17-PLN/ Total PLN
Control EV
Gadlor EV
H
Arrhythmic CMs %
WT
Gadlor-KO
I
WT (1w TAC)
Gadlor - KO (1w TAC)
Sarcomere length (μm)
Time (s)
J
1 week TAC
WT
KO
Normalized Calcium
Time (s)
K
Calcium Parameters (1w TAC)
Calcium Peak Height (AU)
Tau (s)
WT
Gadlor-KO
L
Contractility Parameters (1w TAC)
Sarcomere shortening (%)
Time to 90% relaxation (s)
0.0679
WT
Gadlor-KO
O
Sarcomere Shortening
(%)
KN93
Control EV
Gadlor EV
M
Contractility Parameters (1w TAC)
Sarcomere shortening (%)
Time to 90% relaxation (s)
Control EV
Gadlor EV
N
Calcium Parameters (1w TAC)
Calcium Peak Height (AU)
Tau (s)
ns
Control EV
Gadlor EV
P
Tau (s)
KN93
Control EV
Gadlor EV

Figure 7. *Gadlor* lncRNAs bind to calcium/calmodulin-dependent protein kinase type II in cardiomyocytes.

A. Experimental scheme of RNA-antisense purification coupled with mass spectroscopy (RAP-MS) to identify specific interaction partners of Gadlor1/2 in HL1 cardiomyocytes treated with βgal or Gadlor1/2 adenovirus. **B.** Volcano plot indicating the identified interaction partners of Gadlor1 and Gadlor2 in cardiomyocytes with RAP-MS (Fold change enrichment (FC) threshold 1.2 and p-value < 0.05). UV crosslinking was used to stabilize protein:RNA interactions and non-crosslinked (N-XL) samples were used as background and removed from crosslinked (XL) samples for each indicated condition. **C.** RNA immunoprecipitation (RIP) performed with anti-IgG or anti-CaMKII antibodies from HL-1 cardiac muscle cell lysate to validate the interaction with Gadlors. RT-qPCR analysis showing the enrichment of Gadlor1 and Gadlor2 compared to IgG controls. Data was normalized to input RNA expression. (n=3 for each condition) **D-E.** Exemplary Western blots of phospho-Thr17-PLN and total PLN with CSQ as loading control in (D) WT and Gadlor-KO and (E) in control-EV and Gadlor-EV treated mouse heart tissue samples after 2 weeks TAC**. F-G.** Quantification of Western-blots. **H.** Percentage of isolated adult WT and Gadlor-KO cardiomyocytes with arrhythmic phenotype after 1-week TAC recorded by Multicell HT system (Ion-Optix) Cell number≥30 in each condition. **I.** Exemplary traces of sarcomere shortening (contractility) of adult WT and *Gadlor*-KO cardiomyocytes isolated after 1 week of TAC (1w TAC). Images showing the measurement of transients in WT-CMs in which no arrhythmia was detected, and detection of arrhythmic beating showed as a secondary peak indicating an after-contraction before the end of the first contraction has been reached in GADLOR-KO-CMs. Recordings of transients (nine transient in each measurement cycle) are obtained from a single cardiomyocyte. Images were analysed with the CytoSolver Transient Analysis Tool. **J – N.** Sarcomere contractility and calcium transient measurements were recorded in parallel with Multicell HT system with continuous perfusion of basal media on isolated adult CMs after 1-week TAC. **J.** Representative calcium transient recordings of WT and Gadlor-KO mice shown as normalized levels of calcium (%). **K.** Calcium parameters including calcium peak height (arbitrary units, AU) and decay time (tau, seconds). **L.** Contractility parameters including sarcomere shortening (%) and relaxation. **M.** Sarcomere function and **N.** calcium transient and decay time constant (tau). Recordings were obtained from adult cardiomyocytes isolated from WT mice after 1 week TAC followed by incubation of control-EV (Ad.β*gal*) and *Gadlor1/2*-EVs (Ad.*Gadlor1* and Ad.*Gadlor2*) for 4-6 hours. **O-P.** Sarcomere contractility and calcium tau measurements in cardiomyocytes as described before with and without addition of the CamKII inhibitor KN93. Data are shown as mean±SEM. Data normality was evaluated with Shapiro-Wilk test and p-values were calculated with Student's t-test (Mann-Whitney for non-parametric) for comparing two groups. *p-value<0.05, **p-value<0.01, ***p-value<0.001, ****pvalue<0.0001.

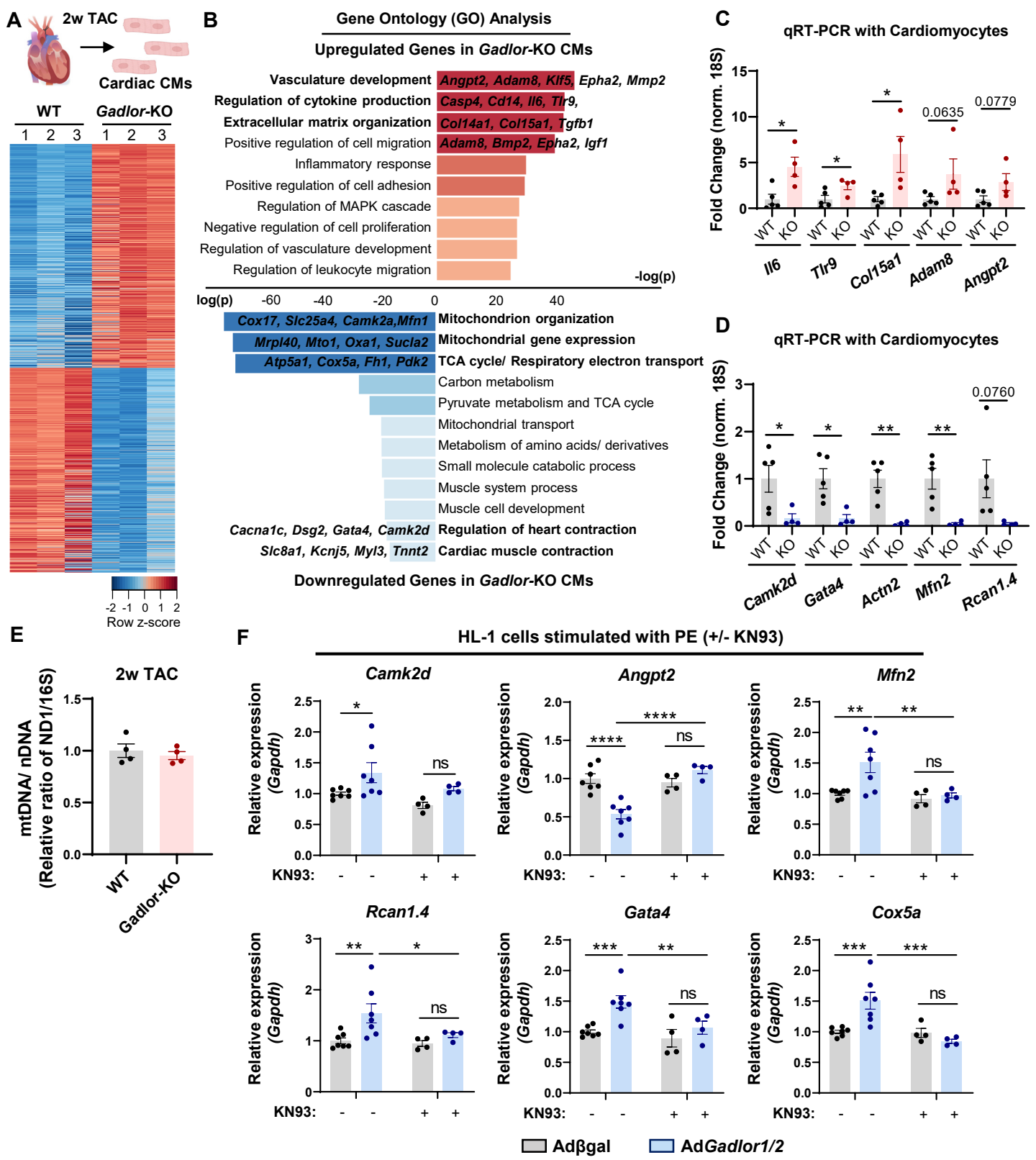

Figure 8. Deletion of *Gadlor1* and *Gadlor2* affects gene expression in cardiomyocytes.

A. Heatmap showing differentially regulated genes analysed by bulk RNAseq of isolated cardiomyocytes after 2-weeks TAC. **B.** Bar plots showing the gene-ontology (GO) analysis of upregulated and downregulated genes in Gadlor-KO CMs after 2-weeks TAC. (Red: Upregulated in Gadlor-KO, Blue: Downregulated in Gadlor-KO). Exemplary genes were listed for selected GO-terms. **C-D.** Validation of selected upregulated and downregulated genes from RNAseq data with qRT-PCR. **E.** Analysis of mitochondrial DNA (mtDNA) to nuclear DNA (nDNA) ratio determined via quantitative PCR by using WT and Gadlor-KO heart tissue samples isolated 2-weeks after TAC. Assessment of ND1 and 16S DNA abundance was used to determine the mtDNA/ nDNA ratio. **F.** qRT-PCR of selected genes in HL-1 cardiac muscle cells overexpressing Gadlor lncRNAs after Gadlor1/2 adenovirus treatment (βgal as control) followed by phenylephrine (PE) stimulation (100 µM, 24 hours) with and without KN93 (1 µM, 2 hours) addition. Data are shown as mean±SEM. Data normality was evaluated with Shapiro-Wilk test. *p*-values were calculated with Student's t-test for parametric (or Mann-Whitney for non-parametric) for comparing two groups. Two-way ANOVA with Fisher's LSD post-hoc test was applied for grouped analysis. ns: no significance, *p-value<0.05, **p-value<0.01, ***p-value<0.001, ****p-value<0.0001.

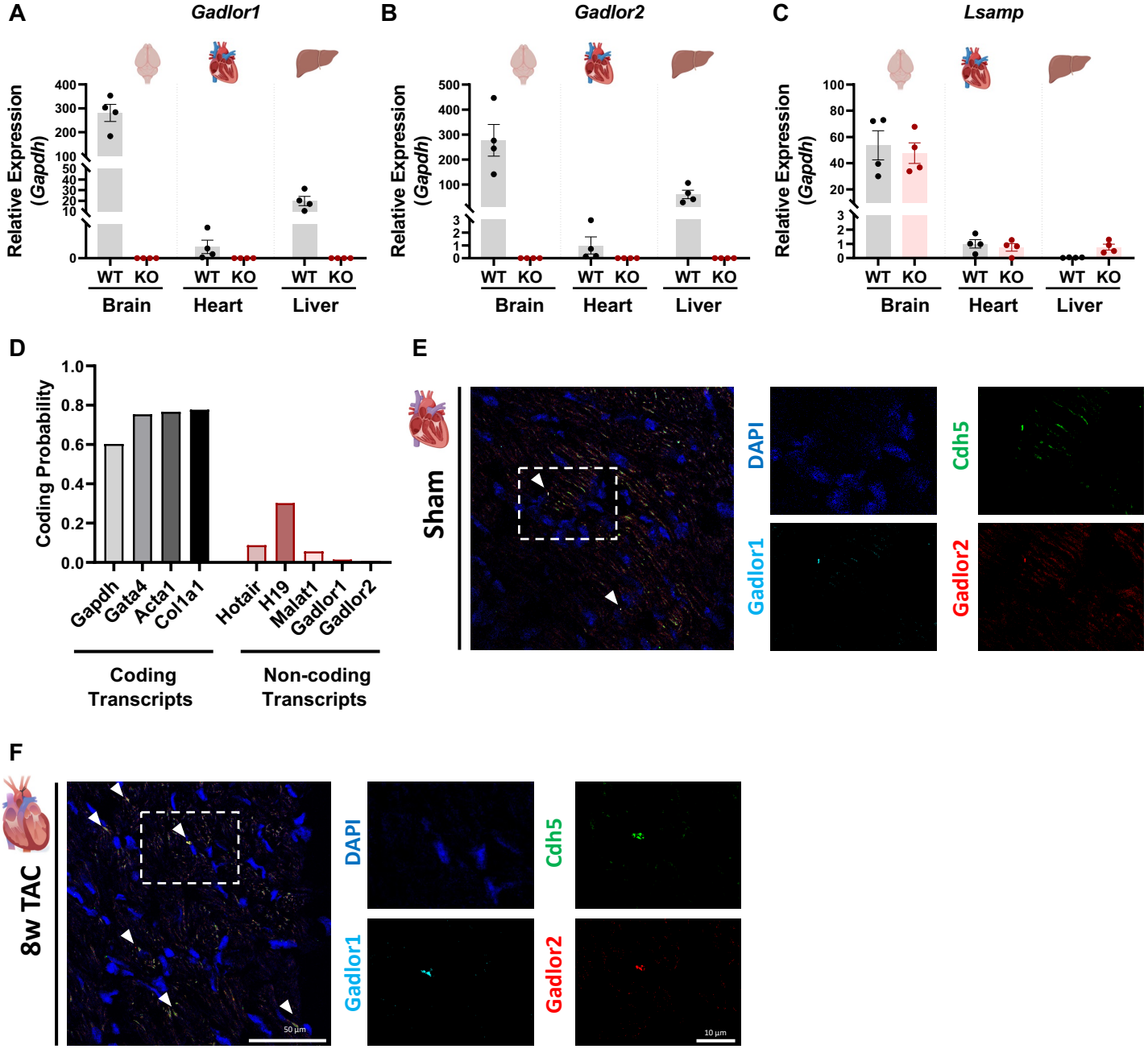

Extended Data Figure 1: *Gadlor1* and *Gadlor2* are non-coding transcripts that are located in the intronic region of the *Lsamp* gene.

A-C. Systemic deletion of the whole region containing *Gadlor* lncRNAs did not affect the expression of the neighbor gene *Lsamp,* which is mainly expressed in brain tissue. (*Gapdh* expression used for normalization) Relative expression of *Gadlor1, Gadlor2* and *Lsamp* were shown in mouse brain, heart and liver tissue samples collected from WT and *Gadlor*-KO mice (n=4, same samples were indicated in each graph). **D.** Coding probability of *Gadlor1* and *Gadlor2* was evaluated with the online Coding Potential Assessment Tool (CPAT - http://lilab.research.bcm.edu/) and compared with coding transcripts and well-known lncRNAs for validation that revealed *Gadlor1* and *Gadlor2* are non-coding transcripts. **E-F.** Fluorescent *in situ* hybridization of *Gadlor1* (cyan), *Gadlor2* (red) and *Cdh5 RNAs* in mouse heart tissue sections of **E.** sham and following **F.** 8-weeks of TAC surgery. *Cdh5* shows endothelial cells (green), nuclei stained with DAPI (blue), and the overlap in 3 channels was indicated with arrows. Dashed rectangles were the zoomed areas showed in separate pictures. Scale bars: 50 μm and 10 μm, as indicated.

A **AK037972 (*Gadlor1*)**

```
#=======================================
# Aligned_sequences: 2
# Gap_penalty: 10.0
# Extend_penalty: 0.5
#
# Length: 578
# Identity:     268/578 (46.4%)
# Similarity:   268/578 (46.4%)
# Gaps:         259/578 (44.8%)
# Score: 740.5
#=======================================
H   1 AAATTGTCTAGAA-TGTGGCAGTTTAAAAACACATCTACATTGATCTACA     49
      ||||||.||||| ||||||.|||||||.|||.||..||||||||||||.
M   1 AAATTGTTTAGAACTGTGGCACTTTAAAAGCACCTCGGCATTGATCTACT     50

   50 GTCTCAAGGTCCCAC--CTTTGTGTTACTTTTAGAATTTGTAGATGGATG     97
      ..|||.||.||.|||  ||.||||.||||||||||.||||||||||||.
   51 AACTCTAGATCTCACCTCTCTGTGCTACTTTTAGAGTTTGTAGATGGATA    100

   98 TTATTCAGCA-AGGATGACTCATCTACATT-TGGTTTGTCAATTTGTTTT    145
      .|.|.||||| |||| ||.||||||||.|| ||  .||||.|||||||||
  101 CTGTCCAGCAGAGGA-GAGTCATCTACGTTCTG--ATGTCGATTTGTTTT    147

  146 CAAAGATCATA----TGTACATAGCGTCCT----TCGATCTTACTTTCCC    187
      ||.||||||.|    || ||||    ||||    |.|     |||.||||
  148 CAGAGATCAGACACTTG-ACAT----TCCTAGAGTGG-----ACTGTCCC    187

  188 TTTAAAATATGAAACTGATAATGACCTTGAAAAAGAT-------AGAATT    230
      |||||||||||||||...||||||.|||..|.||||||        |.|.||
  188 TTTAAAATATGAAACAAGTAATGGCCTACAGAAAGATTATGATAAAACTT    237

  231 TC----------------------------------------AG------    234
      ||                                        ||
  238 TCCAGTTTTTTGGCTTTTCCCTTCGGCCCTGACTGGATGTGTAGTCTACT    287

  235 --CCACAA-------------------------------------------    240
        ||||||
  288 TCCCACAATCCTGTATGTTACATGGTTCCCTACCCAGACCACTCCCTTTG    337

  241 ----------------------------------------GCATCCCA-    248
                                              ||||.|||
  338 CCCCACCCCAAAAATGGCTACTGGGCTTTCTCAATCATCTTGCATGCCAC    387

  249 ---------------------------------TGAA-------AT----    254
                                       ||||       ||
  388 CCCTCGCCTTCTTTTATGTTTCAGAGTTGTGTGTGAAGAATCACATTAGT    437

  255 --TAATGTATCCATACTTTTAACA--CTA-----GTATAC-----TTTAT    290
        ||.|||||.|.|.||||| |||  |||     ||.|||     |||||
  438 GATACTGTATGCTTTCTTTT-ACAATCTATTTACGTTTACACATATTTAT    486

  291 CTTCTTATTT-CA-AATGCTC--TGTCTCC--------------------    316
      .||..||||| || |.|.|||  |||.|.|
  487 TTTTATATTTACATATTTCTCATTGTTTACCAGTTGGCAATAGTGATATT    536

  317 TT---------CTGTCCA--TTACTTCC    333
      ||         ||.|.||  ||||||||
  537 TTGTGAGCTGACTTTACATTTTACTTCC    564
```

B **AK038629 (*Gadlor2*)**

```
#=======================================
# Aligned_sequences: 2
# Gap_penalty: 10.0
# Extend_penalty: 0.5
#
# Length: 913
# Identity:     656/913 (71.9%)
# Similarity:   656/913 (71.9%)
# Gaps:         130/913 (14.2%)
# Score: 2336.5
#=======================================
H   1 AAAAAGAAAATTTGGA-AGATGCTCAAATAGGA-TTGATAGAGGTTCATT     48
      ||.||.||||||||| || |||.||.|||||| ||| .||.|..|||..
M  34 AAGAATAAAATTTGGACAG-TGCACACATAGGACTTG-CAGGGACTCACA     81

   49 TTGTGTCATATTTT-CGCTTTATATGGATGTTGATATGTTCTCAGAATAA     97
      .||||||||||||| |.||||.||||.||||||||||||.||||||| |
   82 GTGTGTCATATTTTGCACTTTTTATGAATGTTGATATGTTTTCAGAAT-A    130

   98 ATTTATAACTGCAATAGAAAATGGAATGACTATTGATTATTTTTTAGTTA    147
      ||||||||||||||.|||||..|||||.||||||||||..||||||||.
  131 ATTTATAACTGCAATTGAAAACTGAATGGCTATTGATTAAATTTTAGTTT    180

  148 CCCAAACTAATTGTCATATAAAGCTTTGTAAAT-CTTTTA-AAATGAGTA    195
      |..|||||||||.||||||||||||..||||| |||||| |||  ||.|
  181 CAAAAACTAATTGACATATAAAGCTTCATAAATCCTTTTAGAAA--AGGA    228

  196 TGGGTGTAAATTAAAAACGAATTAAAGCAGAGGCTTATAAAGACACT---    242
      ||.||.||||||||||||.|||||.||||.||||||||||| |.|||
  229 TGAGTATAAATTAAAAACTAATTACAGCAAAGGCTTATAAA-ATACTCCA    277

  243 ATCTCCCCTTCAATGGGTTATGTATTTTTGTTGTGTGTTAGGAAGATATC    292
      || |||..|||.|| ||||||.||   .||||||.||.||.||||.|.|.
  278 AT-TCCAGTTCTAT-GGTTATATA---CTGTTGTATGCTATGAAGGTGTT    322

  293 TCTTGATCTCCACACCCAAAACTCCTTCC----------AAATGAACAAA    332
      .|||..|||.|..|..||||||||||.||          |.||||||
  323 CCTTTGTCTTCTTAATCAAAACTCCTGCCATAGAATTAAATATGAAC---    369

  333 GGCCTACACACAAAAATTATTTCAATTGCTAATAGCCAGTTTTTAT----    378
            ||.||||..||||.||||||||||....|.|||.|||
  370 --------CATAAAAGATATTTTAATTGCTAATGATTACTTTATATATAG    411

  379 ------TTTTCAAAAGTAAATGCTTTCTTTTTTTGAAAAGTAAATATAAC    422
            |||||||.||                     |||  .|||||.
  412 TATCCCTTTTCAAGAG----------------------AGT--TTATAAG    437

  423 TATTTTAACAAAGTAAGATTTAAAAA---AAAAAACAACTCAGAAAAAAG    469
      .|||||.|...|||||.|||||||||   ||||||.|||      |.|||
  438 AATTTTTAATCAGTAATATTTAAAAATTTAAAAAAGAAC------AGAAG    481

  470 T--GCCAT------GCAG-AGATAACAGGGCTGATCTGTCTGTTATCTGC    510
      |  |||||      |||| ||| |.||      || ||.|.||||||||.
  482 TGGGCCATGTTAAGGCAGCAGA-ACCA------AT-TGCCAGTTATCTGT    523

  511 AGCCTCTATCCTTACTGTTAACAAGCCTTTTATCTTTGAAGACACTAAAC    560
      |.||||||||||..||.|||.||||||||||.|||.||||||||||||.|
  524 AACCTCTATCCTTGATGCTAATAAGCCTTTTACCTTCGAAGACACTAAGC    573

  561 ATCTGGGATCTAAGCACTGACACCTATTAGTTACAGTGGTTTCCTTTTAC    610
      ||||||||||||||.|.||||||||||||||||||.||||||||||||||
  574 ATCTGGGATCTAAGTAGTGACACCTATTAGTTACAATGGTTTCCTTTTAC    623

  611 CTTTCTAAACTATCTGATAGATAAACCTCCAGGAATCCTACAAAATTAGG    660
      | ||||||.|.||||||||||||||||||||||||||||.||||||||.|.
  624 C-TTCTAAGCAATCTGATAGATAAACCTCCAGGAATCCCACAAAATTGGA    672

  661 CCCTTAATTGACCAAACGAATGTCTGTCTCTCTTTTTCAATCTAAATCAA    710
      ||||||||||||||||.|||||.||||||||||||||.||.|.||||||..|
  673 CCCTTAATTGACCAAATGAATGGCTGTCTCTCTTTTACAGTATAAATTGA    722

  711 AAAG-GAGTTTGCTCCTAGGAG--ATGAGATGATGTACAGTGGAAAAAAA    757
      |||| ||||||||||.|.|||  |.||.||.|..||    |||||.|||
  723 AAAGTGAGTTTGCTCCCATGAGGTAAGACATAACTTA----GGAAAGAAA    768

  758 TATTTCA-GCTGCAACTCCACTGGTAACCGTCAATGTGACCTTATAATCT    806
          ||| ||||..||||||||.|..| |.|.|.||||.||||.||||||
  769 ----TCACGCTGAGACTCCACTTGCCA-CATTAGTGTGCCCTTGTAATCT    813

  807 CCCC-----CCAATTTATTCCCA-AAACAGCTA--CCAAAGTGATCTTTC    848
      |.||     |||       |||| .||||| ||  .|||||||||..|||
  814 CACCAAAAGCCA-------CCCACCAACAG-TAGGACAAAGTGATTCTTC    855

  849 TAAAACCCACATC    861
      ||||||.||||||
  856 TAAAACGCACATC    868
```

C

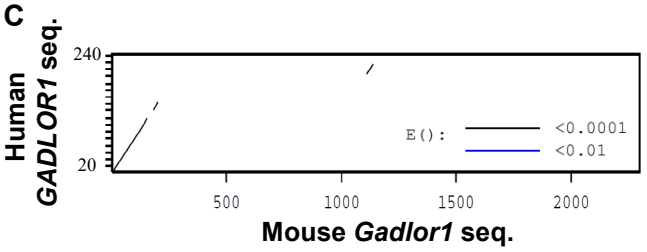

D

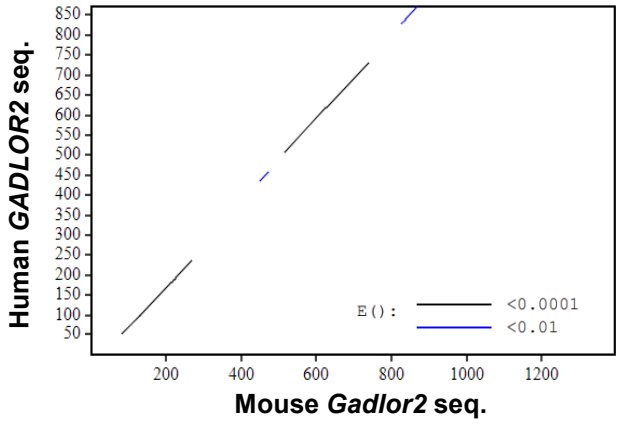

Extended Data Figure 2: Conservation levels of *Gadlor1/2* between mouse and human genome.

A-B. Assessment between human (H) and mouse (M) *Gadlor1/2* in sequence conservation level evaluated with EMBOSS-Water local alignment tool (https://www.ebi.ac.uk/Tools/psa/emboss_water/), and **C-D.** visualization of pairwise local alignment with LALIGN DNA:DNA tool of University of Virginia (https://fastademo.bioch.virginia.edu/fasta_www2/fasta_www.cgi?rm=lplalign).

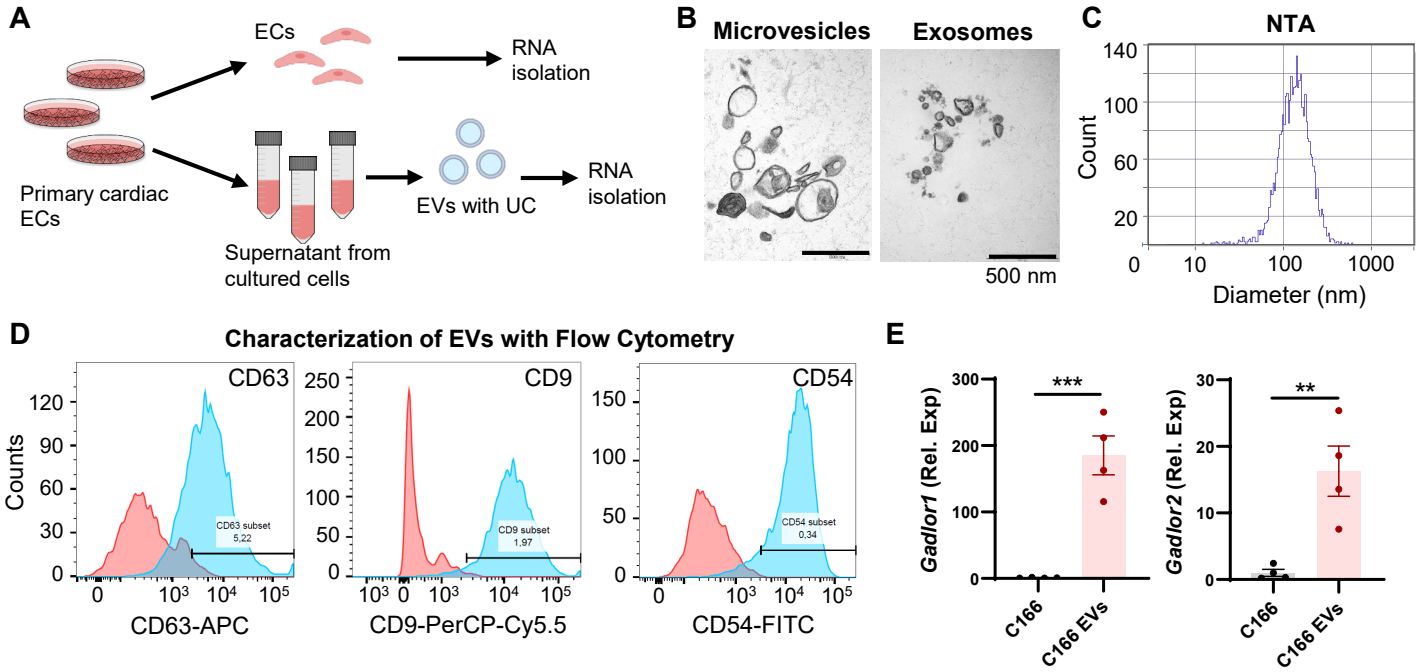

Extended Data Figure 3: *Gadlor* lncRNAs are mainly secreted in endothelial cells (EC) derived extracellular vesicles (EVs).

A. Scheme depicting the experimental design of EV isolation with ultracentrifugation (UC) from cultured primary cardiac ECs. Characterization of cardiac EC-derived EVs by **B.** visualizing microvesicles and exosomes with electron microscopy (scale bar: 500 nm) and **C.** detecting the size in diameter (nm: nanometers) with Nanoparticle Tracking Analysis (NTA). **D.** Flow cytometry analysis of EV surface markers (CD63-APC, CD9-PerCP-Cy5.5 and CD54-FITC) on EC-derived EVs that were stained against markers (blue curve) and compared to isotype control (red curve). **E.** Expression of *Gadlor1* and *Gadlor2* in C166 mouse endothelial cell and in EVs derived from these cells. Data are shown as mean±SEM. Data normality was evaluated with Shapiro-Wilk test and p-values were calculated with Student's t-test for parametric (or Mann-Whitney for non-parametric) assessment. *p-value<0.05, **p-value<0.01, ***p-value<0.001.

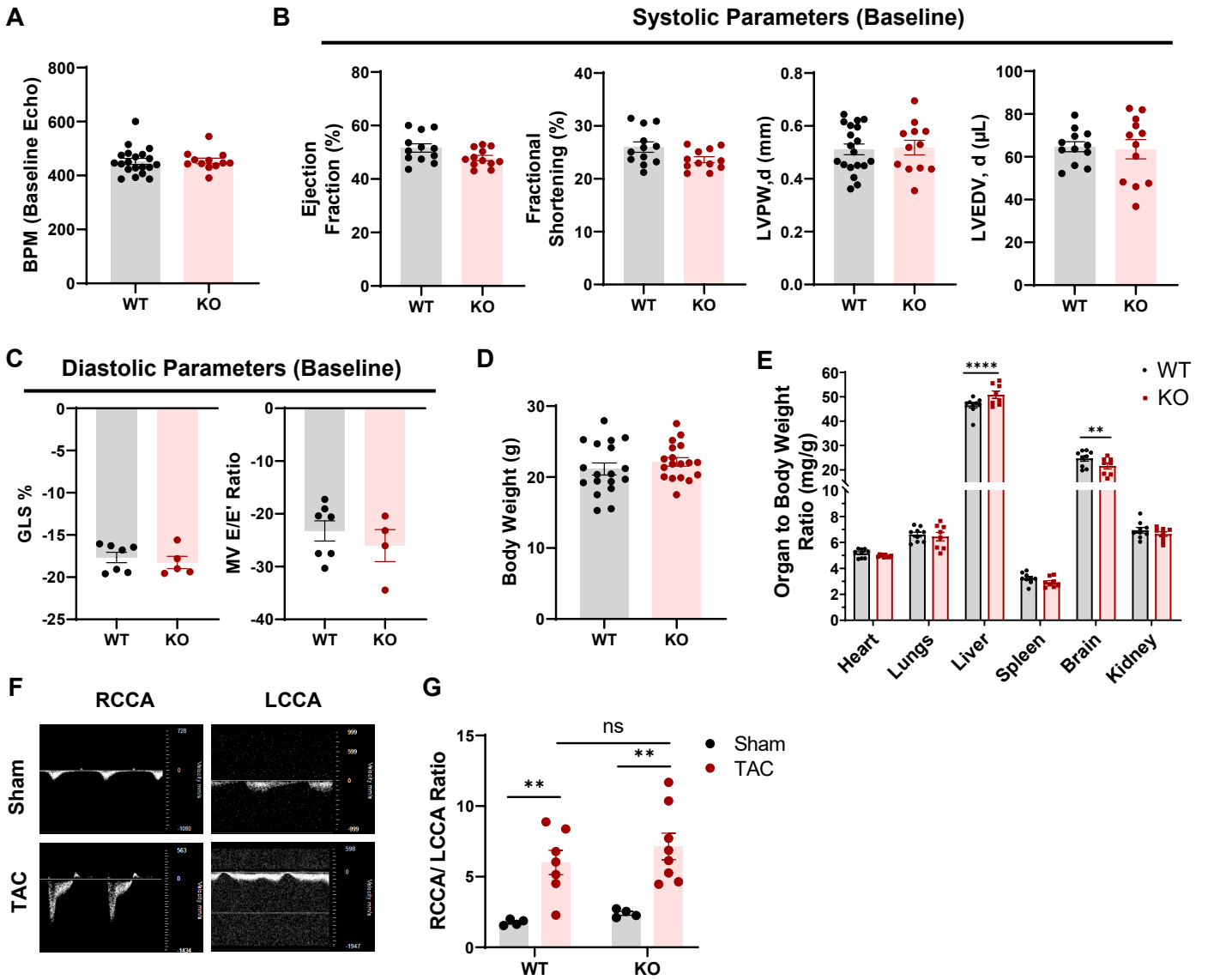

Extended Data Figure 4: Baseline phenotypic characterization of *Gadlor*-KO mice compared to wild-type (WT) littermates.

A. Heart rate of WT and *Gadlor*-KO mice during echocardiography (BPM: beats per minute, n≥12). **B.** Analysis of systolic function parameters of left ventricle (LV) ejection fraction (%), fractional shortening (%), LV posterior wall thickness in diastole (mm) and LV end diastolic volume (µl) (n≥12). **C.** Analysis of diastolic function parameters, global longitudinal strain (GLS, %) and mitral valve (MV) E to E' ratio (n≥4). **D.** Body weight (g) of adult (9 weeks old) WT and *Gadlor*-KO animals (n≥18), and **E.** organ to body weight ratio (mg/g) of isolated organs including heart, lungs, liver, spleen, brain and kidney (n≥8). **F-G.** Representative images and quantification of flow measurement in right and left common carotid arteries (RCCA and LCCA) in sham (n≥4) and TAC (n≥7) mice to measure the strength of aortic constriction in WT and *Gadlor*-KO animals.

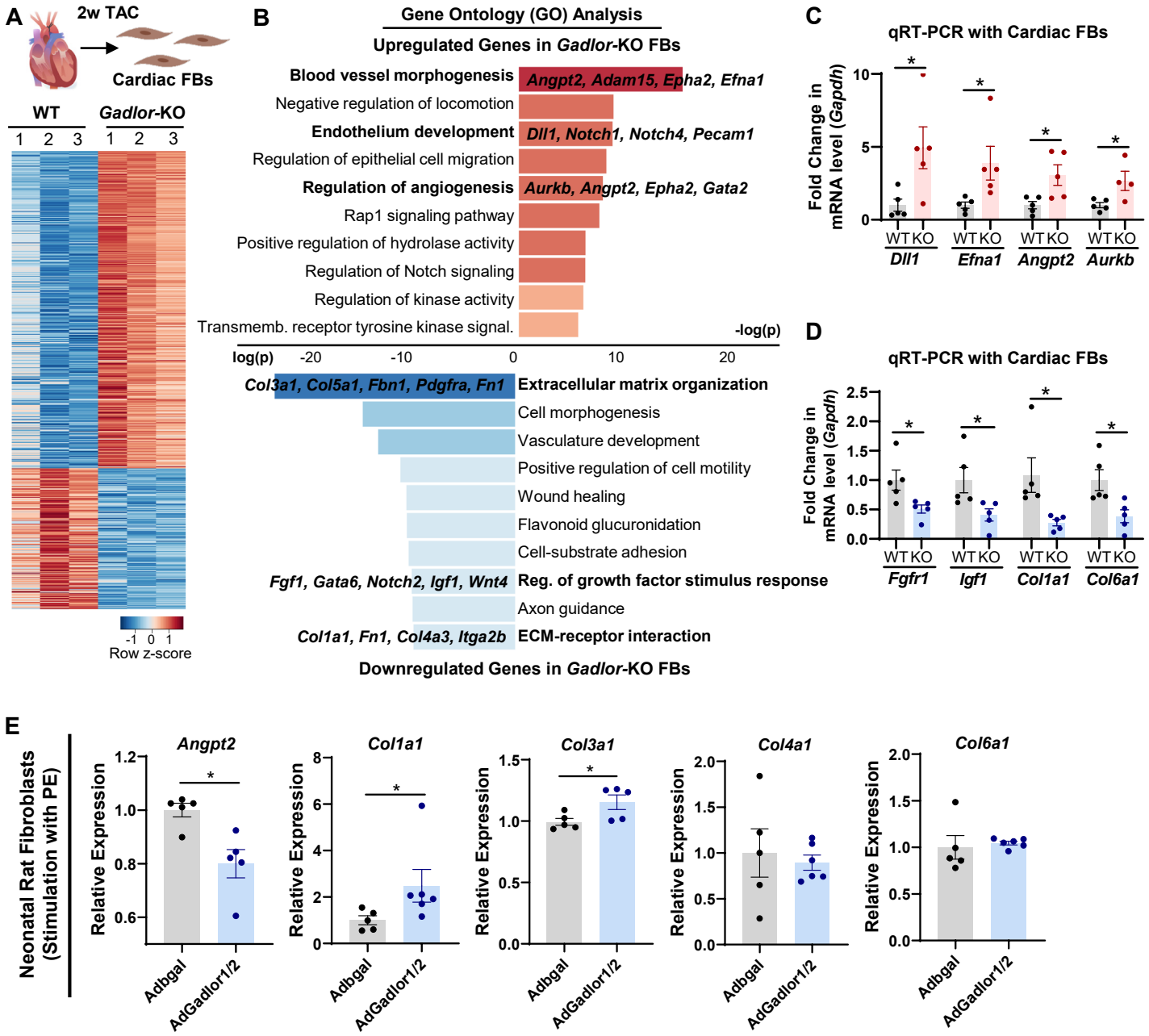

Extended Data Figure 5: RNA sequencing of *Gadlor*-KO cardiac FBs showed less induction of fibrosis-associated genes after TAC.

A. Heatmap showing differentially regulated genes analysed by bulk RNAseq of isolated cardiac fibroblasts after 2-weeks TAC. **B.** Bar plots showing the gene-ontology (GO) analysis of upregulated and downregulated genes in *Gadlor*-KO FBs after 2-weeks TAC (Red: Upregulated in *Gadlor*-KO, Blue: Downregulated in *Gadlor*-KO). Exemplary genes were listed for selected GO-terms. **C-D.** Validation of selected genes from RNAseq data with qRT-PCR in isolated adult cardiac FBs after 2 weeks of TAC (Red: Upregulated in *Gadlor*-KO, Blue: Downregulated in *Gadlor*-KO). **E.** qRT-PCR of selected genes in neonatal rat fibroblasts (NRFB) overexpressing *Gadlor* lncRNAs after *Gadlor1/2* adenovirus treatment (*βgal* as control) followed by phenylephrine (PE) stimulation (100 µM, 24 hours). Data are shown as mean±SEM. Data normality was evaluated with Shapiro-Wilk test and p-values were calculated with Student's t-test for parametric and Mann-Whitney test for non-parametric assessment. *p-value<0.05.

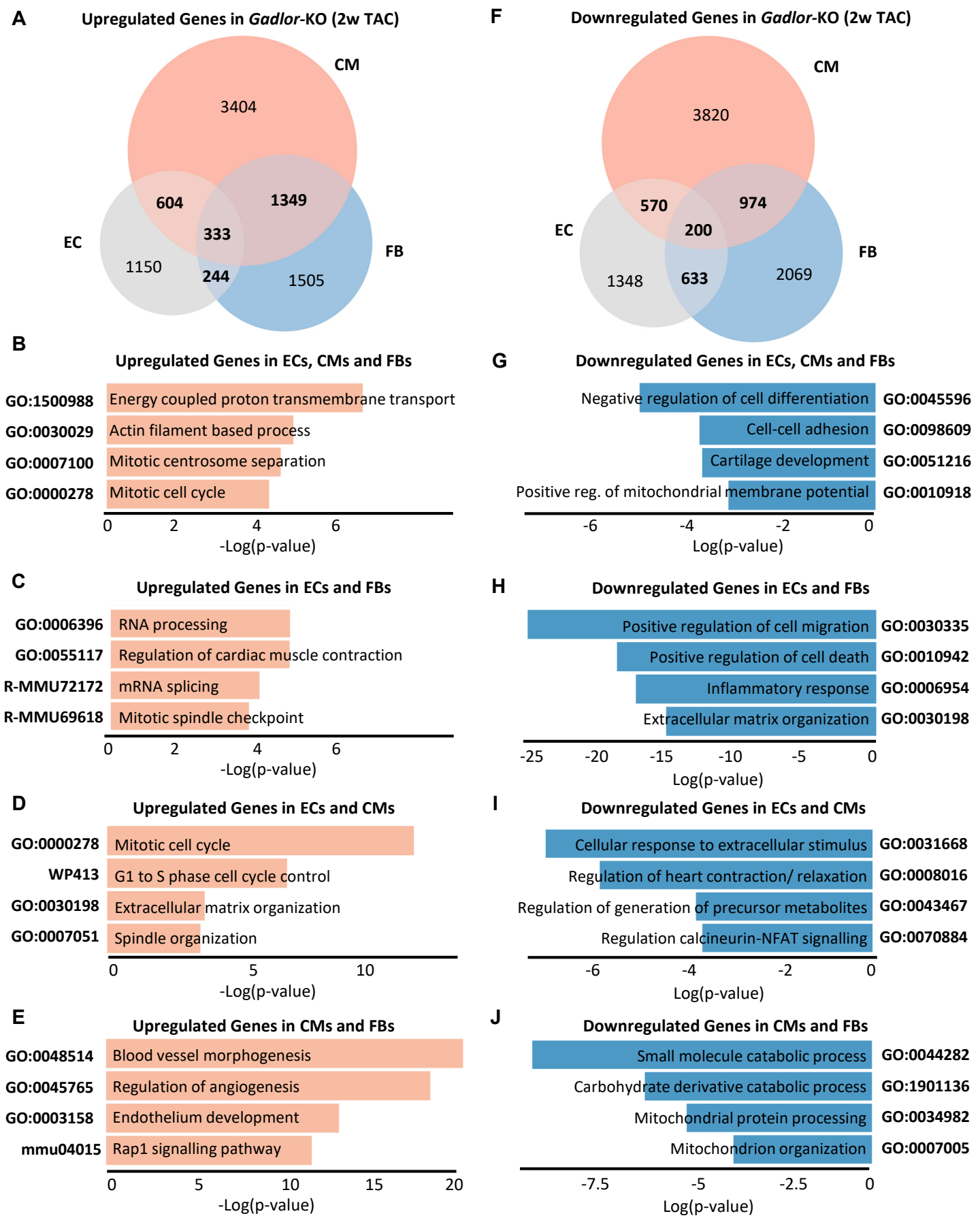

Extended Data Figure 6: Venn diagrams of differentially expressed genes in different cardiac cell types of *Gadlor*-KO mice compared to WT littermates after 2 weeks of TAC. A. Venn diagram of upregulated genes in different cardiac cell types (CM: red, EC: grey, FB: blue) of *Gadlor*-KO mice compared to WT after 2-weeks TAC. The numbers indicating the number of genes in corresponding cell types. Genes were filtered as fold-change greater or equals to 1.2 for each condition. **B-E.** Gene ontology (GO) analysis of indicated intersections representing the overlapping upregulated genes in shown cell type of *Gadlor*-KO compared to WT littermates. **F.** Venn diagram of downregulated genes in different cardiac cell types (CM: red, EC: grey, FB: blue) of *Gadlor*-KO mice compared to WT after 2-weeks TAC. **G-J.** Gene ontology (GO) analysis of indicated intersections representing the overlapping downregulated genes in shown cell type of *Gadlor*-KO compared to WT littermates. Bar plots showing selected GO-terms for each condition.

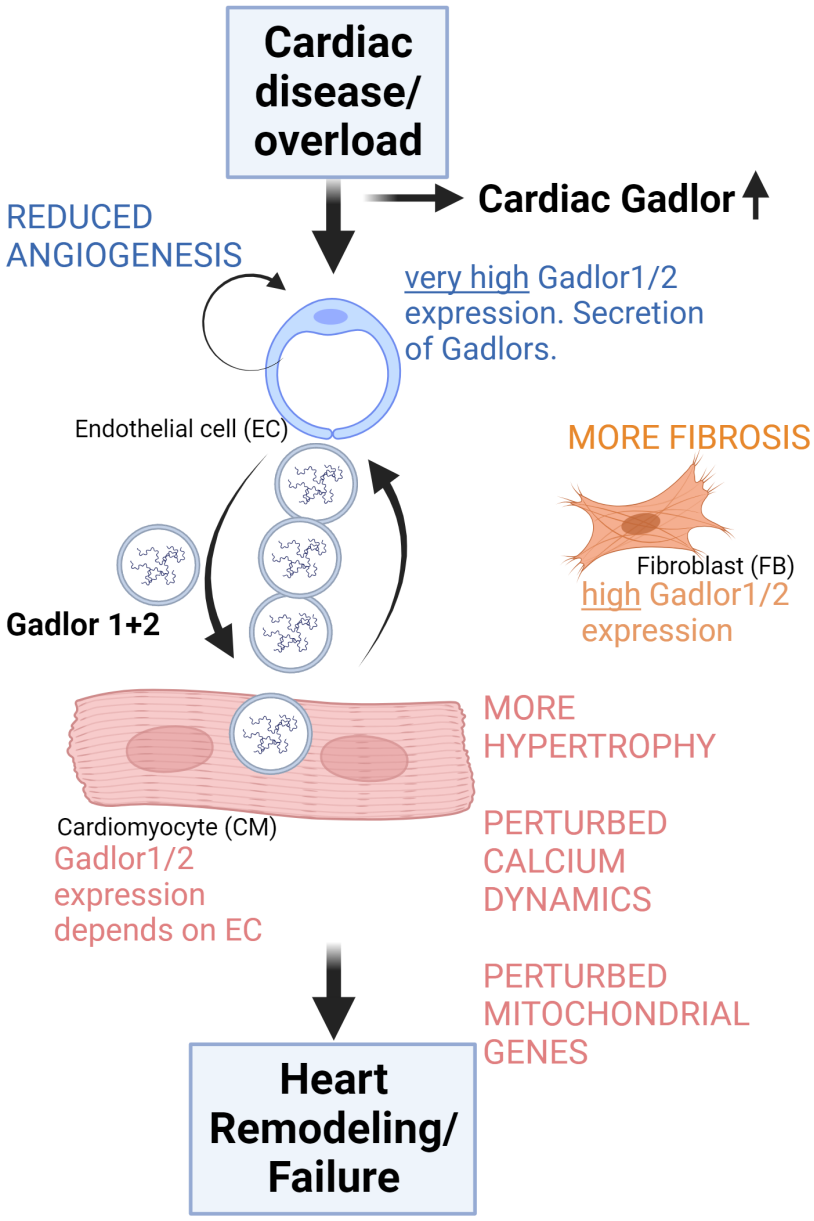

Extended Data Figure 7: Graphical summary showing *Gadlor1* and *Gadlor2* lncRNA expression and their effects (capitalized letters).The illustration was created with BioRender.com.